U.S. DEPARTMENT OF COMMERCE
National Technical Information Service

N66-17325

PARAMETRIC DESIGN STUDY RECUPERATOR DEVELOPMENT PROGRAM SOLAR BRAYTON CYCLE SYSTEM

Airesearch Manufacturing Division
Los Angeles, CA

Mar.64

63

N66-17325

PARAMETRIC DESIGN STUDY
RECUPERATOR DEVELOPMENT PROGRAM
SOLAR BRAYTON CYCLE SYSTEM

NASA CONTRACT: NAS 3-2793

9372

March 10, 1964

Prepared by

A. F. Anderson
S. F. Felszeghy

Edited by: E. F. Busch

Approved: R. D. Mueller
R. D. Mueller

Approved: K. O. Parker
K. O. Parker

GARRETT AIRESEARCH MANUFACTURING DIVISION
Los Angeles, California

CONTENTS

	Page
AXIAL CONDUCTION IN COUNTERFLOW HEAT EXCHANGERS	1
BASIC DATA FOR AXIAL FLOW OUTSIDE TUBE BUNDLES	5
COUNTERFLOW TUBULAR HEAT EXCHANGER DESIGN PROGRAM	7
HEAT TRANSFER MATRIX PARAMETRIC ANALYSIS	13
Multi-Pass Cross-Counterflow Tubular Heat Exchangers	13
Multi-Pass Cross-Counterflow Plate Fin Heat Exchangers	26
Pure Counterflow Tubular Heat Exchangers	32
Pure Counterflow Plate Fin Heat Exchangers	37
COMPARISON AND SUMMARY OF HEAT EXCHANGER TYPES	44
REFERENCES	51

APPENDIX

SMALL SCALE TEST PROGRAM	A-1
Axial Conduction	A-1
Flow Distribution	A-3
Basic Heat Transfer Data for Tubular Matrices	A-4
References	A-8

PARAMETRIC DESIGN STUDY

RECUPERATOR DEVELOPMENT PROGRAM

SOLAR BRAYTON CYCLE SYSTEM

The purpose of this report is to present the results of a parametric design study for the development of a recuperator to be utilized in a closed Brayton cycle space power system which will use solar energy as a heat source and argon as a working fluid. This report concludes the work completed by the AiResearch Manufacturing Division of The Garrett Corporation during the first three months of National Aeronautics and Space Administration Contract NAS 3-2793.

The parametric design study was conducted to provide sufficient data so that optimum recuperator operating conditions may be selected for the Brayton cycle. The study covered a recuperator effectiveness range from 0.75 to 0.95 and a range of $\Delta P/P$ of from 1/2 to 4 percent for both hot and cold flows. The analysis has employed the specified Brayton cycle boundary conditions and gas flow, shown below.

	Temperature, °R	Pressure, psi
Cold Inlet	801	13.8
Hot Inlet	1560	6.73

Gas Flow Rate (each side) = 36.69 lb/min Argon

Four types of heat exchangers were examined. These are, plate fin multipass cross-counterflow, plate fin pure counterflow, tubular multipass cross-counterflow, and tubular pure counterflow. For each type an AiResearch IBM computer program was used to obtain a series of designs over a wide range of problem conditions. For each type of heat exchanger, curves have been prepared to show the change in heat exchanger weight and dimensions for varying effectiveness and pressure drops. The plots include results for the heat exchanger cores only and for the manifolded and packaged cores. Isometric drawings of representative manifolded and packaged cores are also included

AXIAL CONDUCTION IN COUNTERFLOW HEAT EXCHANGERS

The problem of determining the performance of a pure counterflow heat exchanger with heat conduction in the direction of flow was discussed in AiResearch Report L-3895 (Reference 1). Further consideration has been given to this problem. The method of determining the effect of axial conduction in a counterflow heat exchanger presented in Appendix D of the above referenced report has been reevaluated and the following revision made.

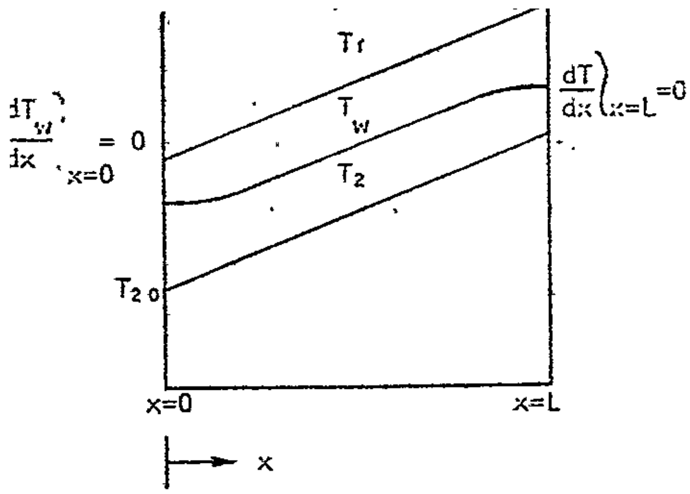

T_1, T_2	temperature of hot, cold fluid
T_W	wall temperature of surface separating hot and cold fluids
C_{P1}, C_{P2}	specific heat of hot, cold fluid
h_1, h_2	film heat transfer coefficient on hot, cold side.
W_1, W_2	flow rate of hot, cold fluid
L	heat exchanger length
A_m	metal area available for heat conduction in direction of flow
hA 2	heat transfer conductance on hot, cold side
	metal thermal conductivity

The conditions of steady state, constant specific heats and constant film heat transfer coefficients were assumed. Also, the thermal resistance of the metal surface separating the hot and cold fluids was assumed to be negligible compared to that of the fluid films. In other words $\frac{\partial T_W}{\partial y} = 0$. The problem thus becomes one-dimensional.

For a differential length Δx of the heat exchanger, energy balance equations may be written for the hot and cold fluids and for the surface separating them. By allowing $Dx \longrightarrow 0$ one obtains the differential equations of temperature distributions,

$$A(T_1 - T_W) = \frac{dT_1}{dx}$$

$$B(T_W - T_2) = \frac{dT_2}{dx}$$

$$D(T_w - T_2) - C(T_1 - T_w) = \frac{d^2 T_w}{dx^2}$$

where $A = \dfrac{(hA)_1}{W_1 C_{p1} L}$ $\qquad$ $B = \dfrac{(hA)_2}{W_2 C_{p2} L}$

$C = \dfrac{(hA)_1}{kA_m L}$ $\qquad$ $D = \dfrac{(hA)_2}{kA_m L}$

By introducing $\dfrac{dT_w}{dx} = u$ the above equations are changed into four first order differential equations. That is, in matrix notation

$$\{T\}' = [M]\{T\}$$

$$\{T\} = \begin{Bmatrix} u \\ T_1 \\ T_2 \\ T_w \end{Bmatrix}$$

and $[M] = \begin{bmatrix} 0 & -C & -D & (D + C) \\ 0 & A & 0 & -A \\ 0 & 0 & -B & B \\ 1 & 0 & 0 & 0 \end{bmatrix}$

Seeking solutions of the form

$$\{T\} = \{K\} e^{\mu x}$$

leads to the characteristic equation

$$\mu \left[\mu^3 - (A - B)\mu^2 - (AB + D + C)\mu + AD - BC \right] = 0$$

If μ_2, μ_3 and μ_4 are the non-zero, real and distinct roots of the expression in brackets above, then the solution of the differential equations is

$$\{T\} = \{K_1\} + \{K_2\} e^{\mu_2 x} + \{K_3\} e^{\mu_3 x} + \{K_4\} e^{\mu_4 x}$$

where $$\left\{K_i\right\} = \lambda_i \begin{Bmatrix} \mu_i \\ \dfrac{A}{A - \mu_i} \\ \dfrac{B}{B + \mu_i} \\ 1 \end{Bmatrix}$$

The coefficients λ_i are determined from the equations which result from the substitution of the boundary conditions into the solution above. Hahnemann (Reference 2) carried this through and then proceeded to find an explicit expression for the heat exchanger temperature effectiveness. His results are rather lengthy and therefore, will not be repeated here. However, it must be pointed out that when the characteristic equation has multiple roots the solution above must be modified according to well established rules. Multiple roots occur for instance when $\frac{A}{B} = \frac{C}{D}$ or when $A = B$ and $C = D$.

The heat exchanger temperature effectiveness was found for the case when $A = B$ and $C = D$, that is, when $W_1 C_{p1} = W_2 C_{p2} = WC_p$ and $(hA)_1 = (hA)_2$. It is

$$E = 1 - \frac{(NC_m + 1)}{(1 + N - \text{[illegible]})}$$

where $$C_m = \frac{kA_m}{L W C_p}$$

$$N = NTU = \frac{(UA)}{WC_p}$$

$$\psi = \frac{1}{2p} \left[\frac{\phi + 1}{1 - p} + \frac{\phi - 1}{1 - p} \right]$$

$$p = \sqrt{1 + \frac{1}{NC_m}}$$

$$\phi = \frac{\cosh 2Np - 1}{\sinh 2Np}$$

If thermal conductivity is negligible, the above equation for effectiveness reduces to the familiar equation

$$E = 1 - \frac{1}{1 + N}$$

When $C_m \longrightarrow \infty$, the effectiveness equation becomes

$$\lim_{C_m \to \infty} E = 1 - \frac{1}{\dfrac{\cosh 2N - 1}{\sinh 2N} + 1}$$

And when $N \longrightarrow \infty$, the effectiveness equation is in the limit

$$\lim_{N \to \infty} E = 1 - \frac{C_m}{2 C_m + 1}$$

If in the above equations $N \longrightarrow \infty$ and $C_m \longrightarrow \infty$, $E \longrightarrow 1/2$ as expected.

The effectiveness equation discussed above was verified by comparison with results obtained by G. D. Bahnke and C. P. Howard (Reference 3). Bahnke and Howard used a numerical finite-difference method to calculate the effectiveness of a periodic flow (rotary type) heat exchanger when heat conduction in the direction of flow is allowed for. Their case of "infinite rotor speed" is equivalent to a direct transfer type counterflow heat exchanger.

BASIC DATA FOR AXIAL FLOW OUTSIDE TUBE BUNDLES

A literature search was conducted to obtain either analytical or empirical data on the fluid friction and heat transfer characteristics of gas flow parallel to, and outside of, plain tube bundles. Most of the pertinent papers that were found dealt with the problem of cooling fuel rod bundles in nuclear reactors. As a consequence the test models that were used in gathering the experimental data presented in these papers had relatively low tube spacing to diameter ratios and also flow length to diameter ratios. All of the available experimental data falls in the turbulent flow region. Only a theoretical friction factor expression has been obtained for flows in the laminar region.

Figure 1 gives a summary of these data. Curves (1) are from Kays and London (Reference 4) and they are for gases flowing inside of plain round tubes when the wall temperature is constant. Except for curves (1), all other curves and data points are for flows outside of tube bundles. The data points located within the triangles and circles were obtained from tests conducted at AiResearch. The test conditions were discussed in detail in AiResearch Report L-3895 (Reference 1). It will suffice to mention here that the tubes were arranged in a triangular bundle utilizing an equilateral tube spacing. Curve (2) was calculated from Sparrow's (Reference 5) analytically derived curves and it seems to be in fairly good agreement with the plotted AiResearch data near the transition region.

Curves (3) are Palmer's (Reference 6) data for very closely spaced smooth tubes. The test fluid was air. The test lattice consisted of seven rods spaced in an equilateral cluster within a hexagonel chamber with circumferential segments of tubing attached to the chamber walls to simulate the adjacent rods of a large array. In Reference 7, test data has been correlated for water flowing parallel to a bundle of tubes arranged equilaterally with a center

AIRESEARCH MANUFACTURING D

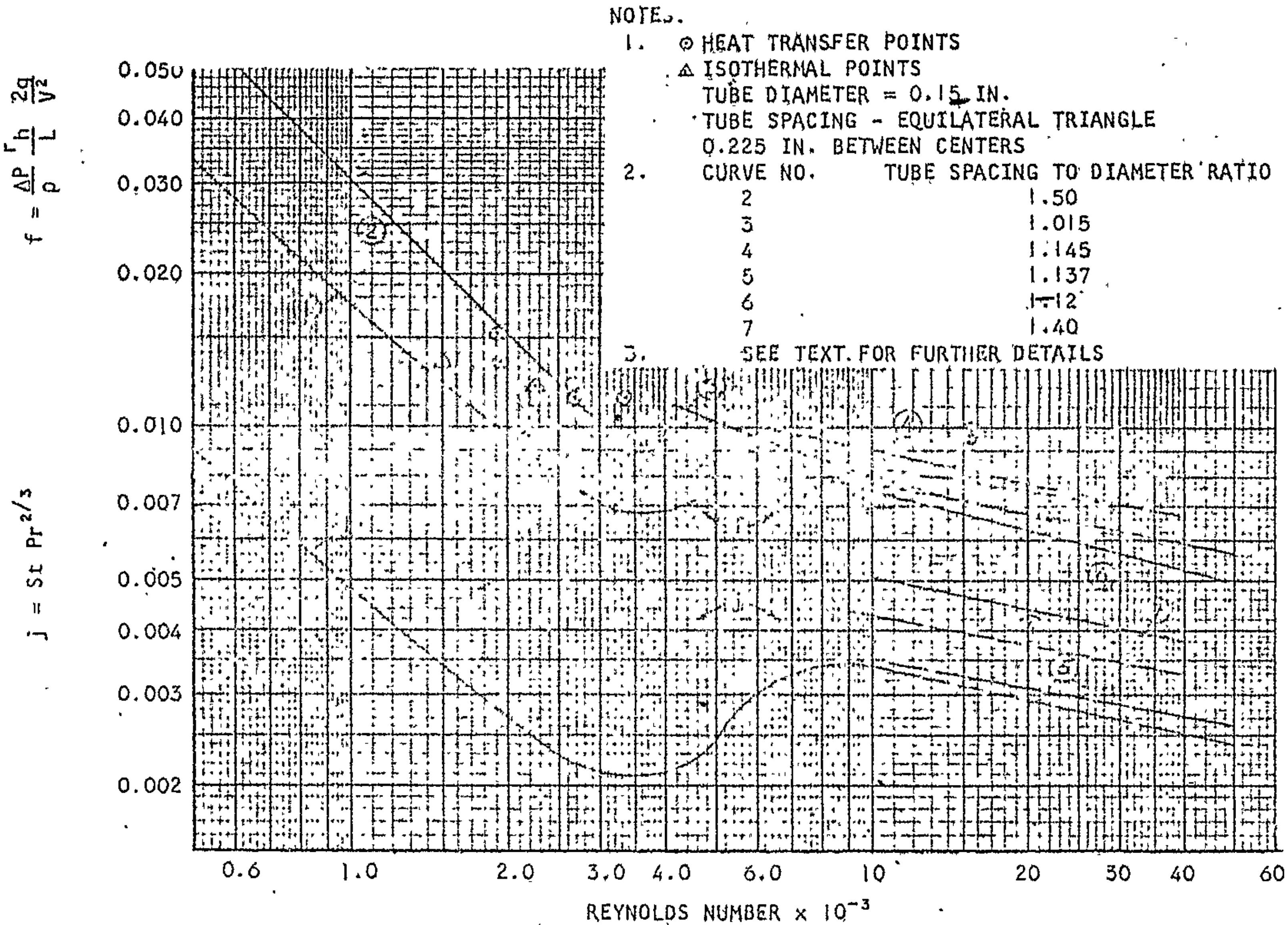

Figure 1. Data for Axial Flow Outside Tube Bundles

spacing to diameter ratio of 1.4. This test core also included tube sections at the outer limits of the tube bundle to simulate a large array. The recommended correlation is

$$j = 0.0205\ Re^{-0.16}\ Pr^{-.209}$$

for Reynolds numbers from 10^4 to 1.2×10^5. The equation is plotted as curve (7). The aforementioned provision of tube sections to simulate large arrays was not made in any of the other tests discussed here.

Curves (4) are Kattchee's (Reference 8) data for a symmetrical and circular cluster of 19 tubes. Equal spacing between all tubes and the channel walls was maintained by means of helically applied spacer wires. The heat transfer data was obtained with air, the friction data with water. Curve (5) is Mackewicz's (Reference 9) data for a symmetrical circular cluster of 19 tubes. The tubes were equally spaced but without mechanical spacers. The test fluid was water. And finally, curve (6) is Le Tourneau's (Reference 10) data. The test core consisted of 19 rods equilaterally spaced to form a hexagonal cluster. A special test section with a hexagonal interior cross section was constructed to accommodate the core. Water was used as the test fluid.

In summary, considerable amount of data is available in the turbulent flow region ($Re > 5000$) and no satisfactory data has been obtained for the fully developed laminar flow region ($Re < 2000$). However, at high effectiveness and low pressure drop conditions the pure counterflow tubular heat exchanger is certainly an attractive possibility. Therefore, laminar flow is of greater interest and AiResearch is planning a small scale test program to obtain data in the low Reynolds number range. An outline of this test program is included in Appendix A.

COUNTERFLOW TUBULAR HEAT EXCHANGER DESIGN PROGRAM

Throughout the parametric analysis four types of heat transfer matrix have been considered, pure counterflow and cross-counterflow plate and fin heat exchangers and pure counterflow and cross-counterflow tubular heat exchangers. At the time of the proposal AiResearch was able to analyze and design heat exchangers of three of those types rapidly and accurately utilizing IBM digital computer programs. No computer program was available at this time to analyze pure counterflow heat exchangers in sufficient detail to permit their accurate design. A program was therefore written for the IBM 7074 Digital Computer which would permit the rapid and accurate evaluation of pure counterflow tubular heat exchangers. This computer program is described briefly below.

Pure counterflow, two fluid heat exchangers are designed by an iteration procedure. Any fluid combination of liquids and gases can be utilized. Five fluid properties for the fluids on both sides are available in the form of Lagrangian tables. These five fluid properties are specific heat, viscosity, Prandtl number, compressibility and density. If the fluid being considered is a liquid, density is estimated from the table and no use is made of the compressibility table. If the fluid is a gas then compressibility may be read from the table and utilized in an equation to calculate gas density. In this case no use is made of the density table. The Lagrangian tables utilized are curves of the particular fluid property versus temperature stored in the computer in the form of pairs of points. When utilizing these tables the computer interpolates between the stored values to determine the fluid properties at the actual temperatures required. In addition to being able consider bundles of plain round tubes the computer program is capable of analyzing surfaces with longitudinal fins on the outside of the tubes and turbulators inside the tubes. Heat transfer and friction factor data for both inside and outside the tube bundle is fed into the machine in the form of Lagrangian tables of Reynolds number versus Colburn modulus and Reynolds number versus Fanning friction factor. In all designs formulated by this computer program the effect of axial conduction on heat exchanger performance is calculated. An option is available in the input to this program as to whether or not it is desired to resize the heat exchanger where the effect of axial conduction is appreciable.

Problem condition input parameters required include flow rate, inlet temperature, inlet pressure and pressure drop available on both sides of the heat exchanger. It is also necessary to specify either effectiveness on one side of the heat exchanger or total heat rejection required. Pressure drops may be specified either in psi or as a percentage of the inlet pressures. The fluid properties are evaluated at bulk average temperatures and gas densities are calculated on the basis of the perfect gas law, but as mentioned above compressibility factors (Z) can also be utilized. Bulk average temperature was selected as in all designs formulated for solar Brayton cycle applications the flow regime within the heat exchanger is laminar. The program designs only the actual heat transfer matrix and the computer does not formulate manifolding or packaging concepts. Allowances are, however, made for shock losses at the entrance and exit of the tube bundle and momentum pressure losses on both sides of the heat exchanger are calculated.

In addition to supplying the heat transfer and pressure drop characteristics of any surface being analyzed in the form of Lagrangian tables, other surface property parameters are required. The surface input information required includes tube diameter, tube spacing, number of fins and fin height (where fins are utilized) and all material thicknesses. Material densities and thermal conductivities are also supplied in order to determine the weight, fin effectiveness and axial conduction parameters for the heat exchanger design. Options are available as to the type of overall heat exchanger configuration required. Basically the program merely sizes the heat exchanger in terms of the number of tubes required and the length of tubes required. It is, of course, possible to arrange this tube bundle into almost any shape and still have a heat exchanger with the same performance capability. Heat exchanger face area may, therefore, be expressed either in terms of aspect ratio or in terms of one controlling dimension.

Output data from this computer program is available in two forms. Both of these forms clearly specify the problem conditions being examined, that is, flow rates, temperatures and pressures. In the short form output all the information that is specified, is the surface geometry being considered and the actual solution obtained with this geometry. This type of output form is shown in Figure 2. The second or long form of output that is available is shown in Figure 3. This long form output shows the same information as the short form output but has a number of additional quantities also shown. These additional

COUNTERFLOW HEAT EXCHANGER BRAYTON CYCLE RECUPERATOR

LEQ= 3 , LP= 1

	INSIDE	OUTSIDE
FLOW(LB/SEC),	WI	WO
	0.61150	0.61150
INLET TEMPERATURE(DEG R)	TI1	TO1
	801.00000	1560.00000
OUTLET TEMPERATURE(DEG R)	TI2	TO2
	1522.05600	838.94290
INLET PRESSURE(PSIA)	PI1	PO1
	13.80000	6.73000
PRESSURE CRC	CPI	CPO
	1.00000	1.00000
EFFECTIVENESS	EI	EO
	0.95000	0.95000
HEAT REJECTION(BTU/SEC)	QX	
	24.7184	

SUMMARY OF SOLUTIONS

FACE ASPECT RATIO= 1.00000

TUBE DIA (IN.)	SPACING		NO. OF FINS	FIN HEIGHT (IN.)	SURFACE IN	SURFACE OUT	NO. OF TUBES	TUBE LENGTH (IN.)	FACE DIMENSION (IN.)	WEIGHT (LB)	EFF. AXIAL	PRESSURE DROP INSIDE	PRESSURE DROP OUTSIDE
0.2100	1.500	1.500	C.0	0.000	PL TB	PL TB	2874.	274.4	16.887	579.0	0.9494	0.4140	0.1176
0.2100	1.500	1.500	C.0	0.000	PL TB	PL TB	2874.	274.4	16.887	579.0	0.9474	0.4140	0.1176
0.2100	1.250	1.250	C.0	0.000	PL TB	PL TB	4810.	119.4	18.205	421.6	0.9493	0.1064	0.2019
0.2100	1.250	1.250	C.0	0.000	PL TB	PL TB	4810.	119.4	18.205	421.6	0.9493	0.1064	0.2019
0.2100	1.100	1.100	C.0	0.000	PL TB	PL TB	10781.	42.3	23.985	334.5	0.9475	0.0175	0.2019
0.2100	1.100	1.100	C.0	0.000	PL TB	PL TB	11134.	43.9	24.429	359.9	0.9509	0.0175	0.2019
0.1500	1.500	1.500	C.0	0.000	PL TB	PL TB	5861.	138.4	17.225	423.1	0.9493	0.4140	0.1106
0.1500	1.500	1.500	C.0	0.000	PL TB	PL TB	5861.	138.9	17.225	423.1	0.9493	0.4140	0.1106
0.1500	1.250	1.250	C.0	0.000	PL TB	PL TB	9421.	61.9	18.295	304.6	0.9488	0.1131	0.2019
0.1500	1.250	1.250	C.0	0.000	PL TB	PL TB	9676.	62.[illegible]	18.444	314.6	0.9503	0.1131	0.2019
0.1500	1.100	1.100	C.0	0.000	PL TB	PL TB	21293.	21.6	24.077	239.7	0.9445	0.0136	0.2019
0.1500	1.100	1.100	C.0	0.000	PL TB	PL TB	22814.	23.2	24.924	275.2	0.9506	0.0186	0.2019
0.1250	1.500	1.500	C.0	0.000	PL TB	PL TB	4674.	95.0	17.465	355.5	0.9491	0.4140	0.1058
0.1250	1.500	1.500	C.0	0.000	PL TB	PL TB	4674.	95.0	17.465	355.5	0.9491	0.4140	0.1058
0.1250	1.250	1.250	C.0	0.000	PL TB	PL TB	14[illegible].	42.9	18.420	251.5	0.9432	0.1133	0.2019
0.1250	1.250	1.250	C.0	0.000	PL TB	PL TB	14277.	43.[illegible]	18.643	266.2	0.9559	0.1182	0.2019
0.1250	1.165	1.100	C.0	0.000	PL TB	PL TB	36762.	15.0	24.116	199.6	0.9411	0.0195	0.2019
0.1250	1.100	1.100	C.0	0.000	PL TB	PL TB	39418.	17.7	25.435	247.0	0.9592	0.0194	0.2019
0.1000	1.500	1.500	C.0	0.000	PL TB	PL TB	14122.	[illegible]	17.02[illegible]	216.3	0.9447	0.4140	0.0989
0.1000	1.500	1.500	C.0	0.000	PL TB	PL TB	143[illegible].	[illegible]	17.171	235.6	0.9502	0.4140	0.0990
0.1000	1.250	1.250	C.0	0.000	PL TB	PL TB	21[illegible].	[illegible]	[illegible]	[illegible]	[illegible]	0.1267	0.2019
0.1000	1.250	1.250	C.0	0.000	PL TB	PL TB	22[illegible].	29.1	[illegible]	213.2	0.9578	0.1266	0.2019
0.1000	1.125	1.100	C.0	0.000	PL TB	PL TB	49213.	9.6	24.156	159.1	0.9337	0.0207	0.2019
0.1000	1.125	1.100	C.0	0.000	PL TB	PL TB	[illegible]	11.7	24.[illegible]	244.4	0.9479	0.0207	0.2019

Figure 2. Typical Short Form Output from IBM Digital Computer Program

```
INSIDE SURFACE IS  PL TB  OUTSIDE SURFACE IS  PL TB

  TUBE DIA       XT          XL          WALL T      TURB. T      FIN T       FIN HT      NO. OF
   (IN)                                   (IN)        (IN)        (IN)        (IN)        FINS
   0.21000     1.50000     1.50000     0.00400     0.00000     0.00000     0.00000     0.00000

 NO. TUBES    TUBE L      FACE HT      FACE W      ASPECT      WEIGHT      VOLUME      PRESSURE DROP
               (IN)        (IN)        (IN)                    (LB)      (CU. FT.)    INSIDE  OUTSIDE PERCENT
  2874.000   274.44848    16.88706    16.88706    1.00000    578.99741    45.29236    3.00000    1.74783

  PRES DROP,PSI        UAP        DPM       DPSUM       SHOKI       SHOKO      AFACE        ETAI      ETAO
 INSIDE  OUTSIDE                  0.0     (PERCENT)                          (SQ  FT)
 0.4140  0.1176     3.7625    41.7391      4.7478      1.5000      1.5000     1.9804      1.0000  1.0000

    NTHI,         NATC          UA          REI          REO          GI           GO          RHO
 BTU/SEC R    BTU/SEC R    BTU/SEC R                             LB/SEC SQ FT  LB/SEC SQ FT   (FT)      EAX
   4.23607      2.31810      1.51395    585.59352    548.55687     0.95638      0.47437     0.00816    0.94943
```


```
INSIDE SURFACE IS  PL TB  OUTSIDE SURFACE IS  PL TB

  TUBE DIA       XT          XL          WALL T      TURB. T      FIN T       FIN HT      NO. OF
   (IN)                                   (IN)        (IN)        (IN)        (IN)        FINS
   0.21000     1.50000     1.50000     0.00400     0.00000     0.00000     0.00000     0.00000

 NO. TUBES    TUBE L      FACE HT      FACE W      ASPECT      WEIGHT      VOLUME      PRESSURE DROP
               (IN)        (IN)        (IN)                    (LB)      (CU. FT.)    INSIDE  OUTSIDE PERCENT
  2874.000   274.44848    16.88706    16.88706    1.00000    578.99741    45.29236    3.00000    1.74783

  PRES DROP,PSI        UAP        DPM       DPSUM       SHOKI       SHOKO      AFACE        ETAI      ETAO
 INSIDE  OUTSIDE                  0.0     (PERCENT)                          (SQ  FT)
 0.4140  0.1176     3.7625    41.7391      4.7478      1.5000      1.5000     1.9804      1.0000  1.0000

    NTHI,         NATC          UA          REI          REO          GI           GO          RHO
 BTU/SEC R    BTU/SEC R    BTU/SEC R                             LB/SEC SQ FT  LB/SEC SQ FT   (FT)      EAX
   4.23607      2.31810      1.51395    585.59352    548.55687     0.95638      0.47437     0.00816    0.94943
```


ıre 3. Typical Long Form Output for First Two Cases of Figure 2 quantities include mass velocity, Reynolds number and heat transfer conductance on both sides of the heat exchanger. In the examples illustrated in Figures 2 and 3 there are two answers given for each surface considered. The first of these answers is the solution obtained by the program for a heat exchanger without allowing for axial conduction. The second solution is the resized heat exchanger which allows for axial conduction.

The design technique utilized by the computer program is very straight forward. For any given problem condition and specified matrix surface the program determines a minimum number of tubes and tube length required to meet the heat transfer requirements within the allowable pressure drop limits. The program first applies what is known as the impossibility equation to determine the free-flow area for inside the tube bundle. This so-called impossibility equation is a parameter which links the heat transfer and pressure drop requirements of one side of a heat exchanger into a single parameter. The name impossibility equation stems from its most common use which is to determine whether or not it is possible to build a heat exchanger to the given conditions within a specified envelope. Having determined a free-flow area inside the tubes on the tube side of the heat exchanger, the program then calculates the length of tubes corresponding to this free-flow area. With this now established tube bundle, the program next checks whether or not the available pressure drop on the outside of the tube bundle is exceeded. If this allowable pressure drop is exceeded the program then sizes a new tube bundle based on the outside the tubes conditions. Having now determined a tube bundle which does not exceed the allowable pressure drop on either side and which utilizes all the available pressure drop on one side, the program then calculates the heat transfer capabilities of this tube bundle. If this estimated value of the heat transfer capabilities is not sufficient to meet the required problem conditions an adjustment is made to the free-flow area on the controlling side of the heat exchanger and the pressure drop and heat transfer calculations repeated. This process is repeated until a satisfactory solution is found which meets both the heat transfer and pressure drop requirements. The effect of axial conduction on this heat exchanger design is then calculated. The method utilized to determine the effect of axial conduction on this heat exchanger is that determined by AiResearch and described in some detail earlier in this report. At the present time the method utilized by the program is the limited case solution, that is, the case that requires the capacity rates and heat transfer conductances to be the same on both sides of the heat exchanger. As the capacity rate ratio for the recuperator for the solar powered Brayton cycle system is one, this is a valid approximation for calculating the effect of axial conduction in this particular application.

Having determined the effectiveness of the heat exchanger design with the allowance for axial conduction, the program then compares this effectiveness with the effectiveness required. If the two values of effectiveness, that is, the required effectiveness and the calculated effectiveness, do not fall within one tenth of one percent of each other the program then designs a second heat exchanger. As in the previous design iteration, a factor is applied to the controlling side free-flow area, a new tube bundle size is determined and its effectiveness allowing for axial conduction again compared with the required effectiveness. The process is again repreated until a satisfactory solution is determined. All loops (iteration processes) are counted and if no convergence is found within the specified number of iterations the attempt to find a solution for that particular problem is abandoned. When this occurs a message informing the program's user of this failure to converge is printed out together with a solution available in the machine at that time. The program then moves on to the next problem condition. With the finally accepted solution for any problem conduction, heat exchanger weight, actual dimensions, and performance margins (always present due to tolerances or convergence) are estimated and the solutions made available as output data sheets in either the short or long form described above.

The above described computer program was written for the IBM 7074 Digital Computer (an AiResearch in-house facility). Utilizing this program on this machine, it is possible to obtain solution for approximately 25 different matrix surfaces in one minute of operating time. This program can, therefore, be utilized to determine solutions for a large number of surfaces and a large number of problem conditions with minimum usage of either engineering or machine time.

HEAT TRANSFER MATRIX PARAMETRIC ANALYSIS

The object of the parametric analysis was to determine the optimum heat exchanger design for the solar Brayton Cycle recuperator problem conditions specified by NASA. The operating conditions and range of variables to be examined are shown in the introduction section of this report. In order to determine the optimum heat exchanger design for this entire range of operating conditions, AiResearch considered four types of fixed boundary heat exchanger. The four types of heat exchangers considered were. (1) cross counter-flow tubular, (2) pure counter-flow tubular, (3) cross counter-flow plate and fin, (4) pure counter-flow plate and fin. As there is no single, unique heat exchanger which is optimum for satisfying all the specified operating conditions for the recuperator. It was necessary to examine each of the four matrices being considered in detail over at least a part of the specified range. A very large number of matrix geometries were analyzed for each of the four types of heat exchangers. The design and analysis of each type of heat exchanger were conducted by utilizing IBM digital computer programs written by AiResearch specifically to design heat exchangers. Only one new computer program was required in order to examine these matrices. This new program, written specifically for this contract, designs pure counterflow tubular heat exchangers. Each of the four types of heat transfer matrix analyzed is discussed individually below.

Multi-Pass Cross Counterflow Tubular Heat Exchangers

In order to design cross counterflow tubular heat exchangers for the full range of specified cycle conditions, a very large number of heat transfer matrices were considered. Matrix variables that were considered, included different tube diameters, different tube spacings and both plain and ring dimpled tubes. The use of ring dimpled tubes increases the heat transfer on the insider surface of the tubes, but also yields a substantial increase in friction factor. In some heat exchanger designs, however, this type of turbulence promotion can be beneficial. Throughout the analysis, all heat exchangers were assumed to be fabricated from stainless steel and the tube wall thickness was held constant at 0.004 inches.

The initial survey of this type of heat exchanger consisted of taking the specified problem conditions and obtaining heat exchanger cores from the IBM computer program. During this initial survey, the total available pressure drop was utilized in the heat exchanger core. The results obtained from these computer runs are shown in Figures 4, 5 and 6. Figure 4 shows how the weight and basic core dimensions of this type of heat exchanger vary with effectiveness. Curves are shown for three different pressure drop levels. The pressure drop values utilized in Figure 4 were $(\Delta P/P)_{total}$ of 1 percent. 4 percent and 8 percent. At each different effectiveness, a different number of passes was utilized. The number of passes associated with each particular effectiveness is shown on the curve. As the effectiveness is increased, it becomes necessary to increase the number of passes as the effect of no interpress mixing becomes more and more important as effectiveness is increased. At the very high effectiveness (greater than 0.9) even the use of as many passes as 12 does not really approach the idealized condition of pure counterflow. Figures 5 and 6

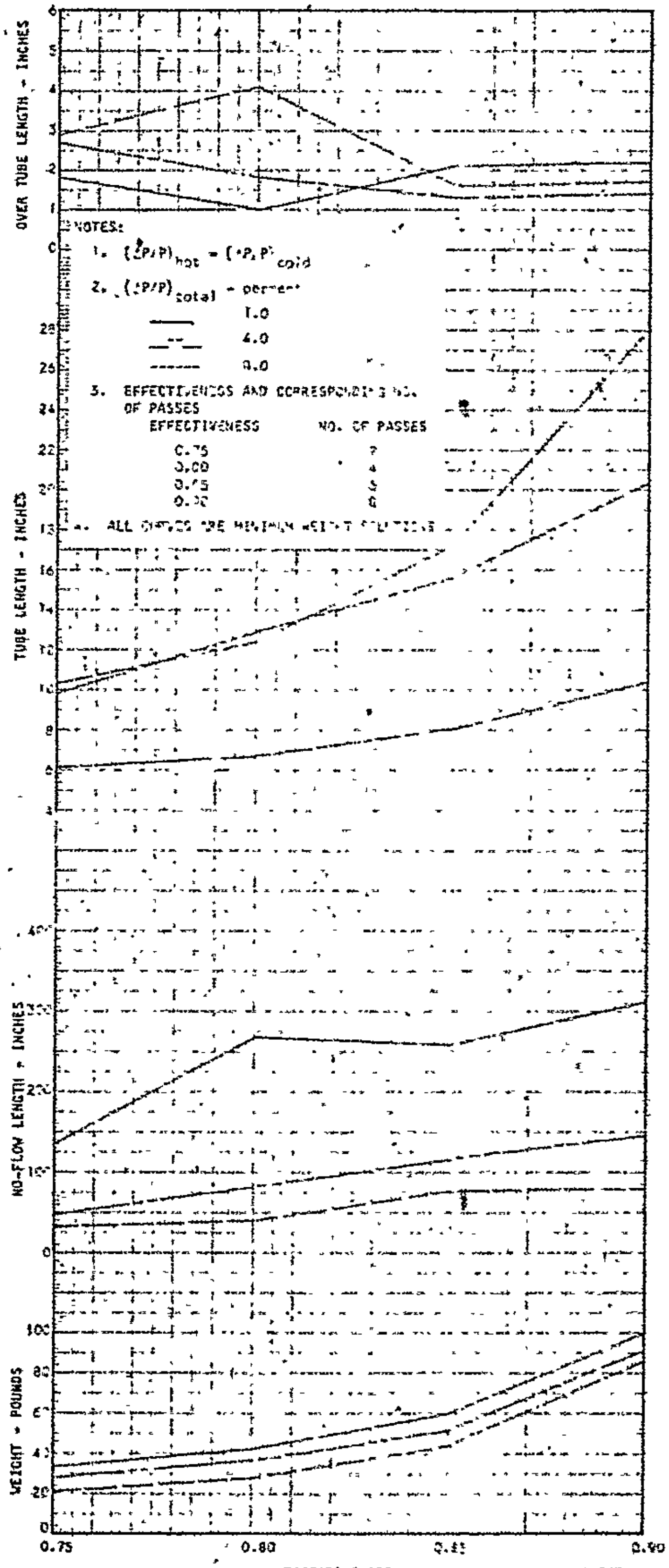

gure 4. Tubular Multipass Cross Counterflow Core Parameters Versus Effectiveness

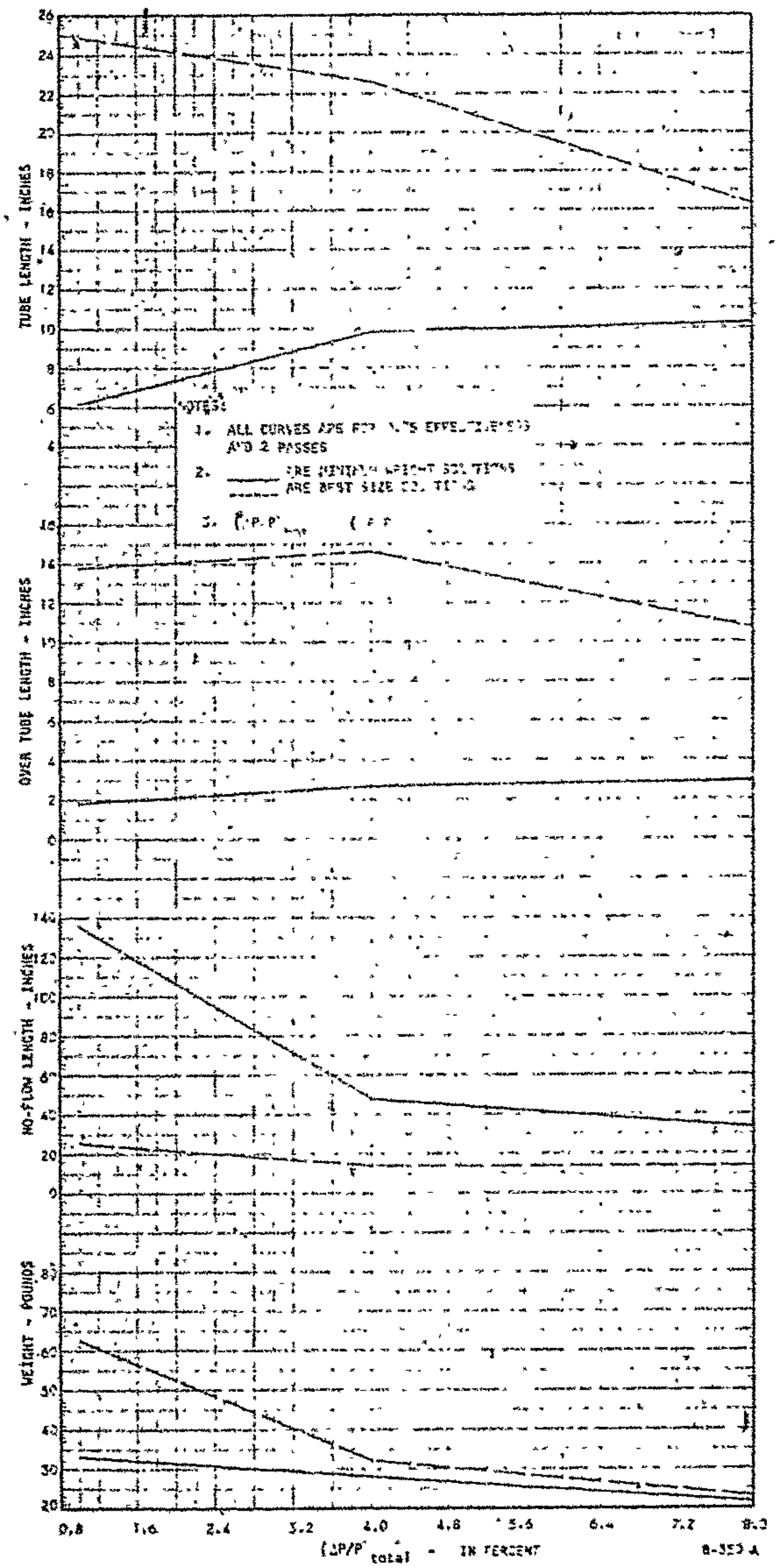

Figure 5. Tubular Multipass Cross Counterflow Core Parameters Versus Percent Pressure Drop

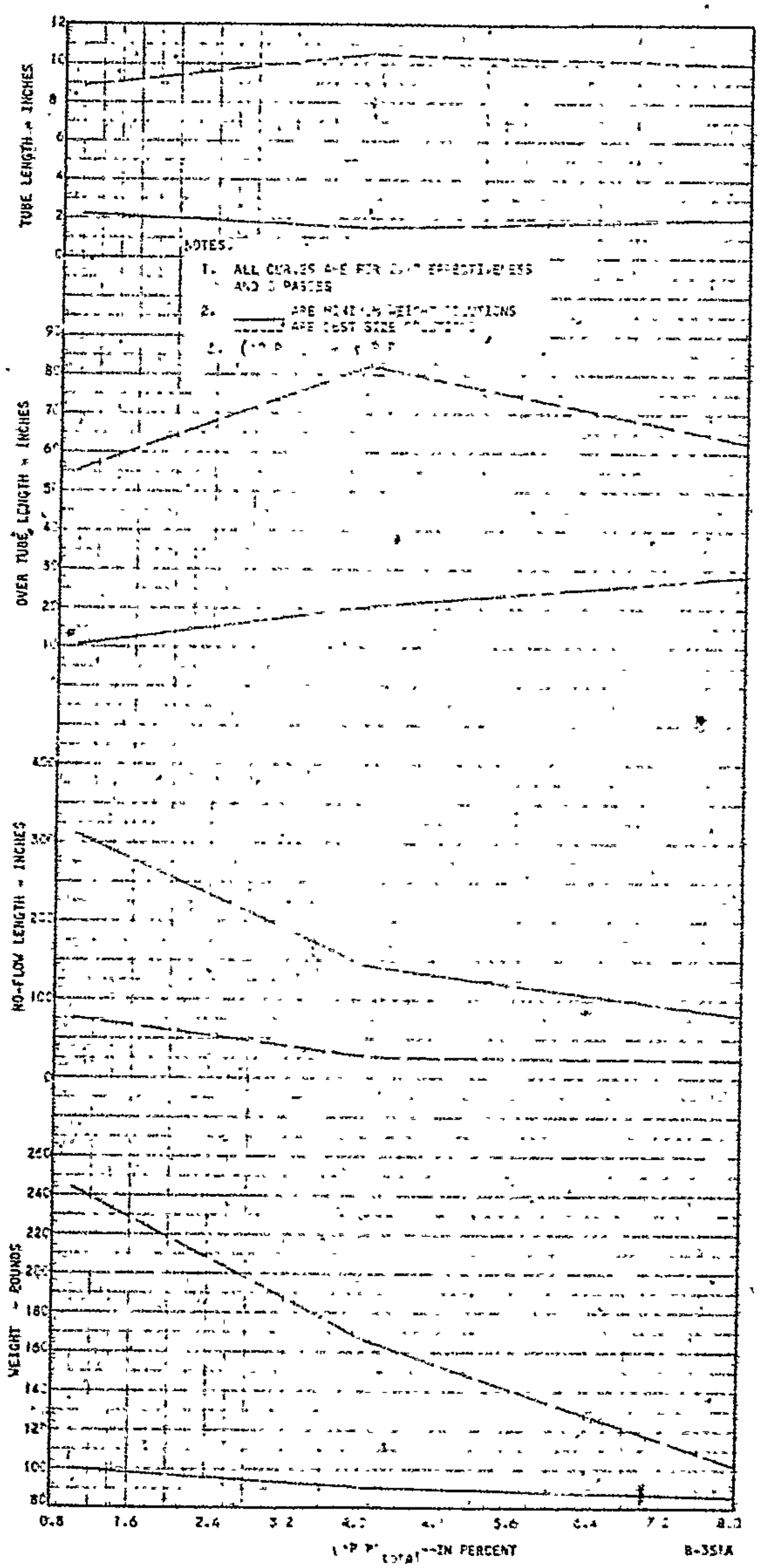

Figure 6. Tubular Multipass Cross Counterflow Core Parameters Versus Percent Pressure Drop

show the effect on weight and core dimensions of varying percentage pressure drops for heat exchanger effectivenesses of 0.75 and 0.90 respectively. On both these figures, curves are shown for minimum weight solutions and best size solutions. The definition of these two terms may best be explained as follows. The curves for minimum weight solutions were obtained by selecting the weights and dimensions obtained from the computer program for the matrix which gives the lightest weight solution for any particular problem. The so-called best size solutions were selected by picking the heat exchanger matrix which came closest to a conventional, rectangular tube bundle. In almost all cases the best size solution resulted in a substantially heavier core than the minimum weight solution. This is particularly true at high effectiveness and low pressure drop. At this end of the range of operating conditions examined, even the so-called best size solutions still result in very long no flow lengths.

The type of curve utilized, to illustrate the effect of either effectiveness or pressure drop on heat exchanger core weight and dimensions, is to connect the actual data points obtained by straight lines. This particular method of presenting the data was selected as in some cases interpolation between the actual data points, is not strictly permissible. This is particularly true of the parameter, tube length. If the curves were prepared utilizing the same matrix geometry throughout, then both core geometry and core weight would give smooth curves for varying effectiveness and pressure drop. However, the same matrix geometry does not always yield either minimum weight or best size solutions and smooth curves are not obtained. If it is desirable to select a core operating at some intermediate condition, the curves shown in Figures 4, 5 and 6 give a very good indication of the expected dimensions and weight, but cannot be utilized to determine exact dimensions and weights.

The second phase of the study of this particular type of heat transfer matrix consisted of examining the various possible packaging methods and re-evaluating pressure losses in the heat exchangers to account for the necessary manifolding. For this particular type of heat exchanger a large number of packaging concepts are available, some of them conventional, some of them less conventional and all of them yielding different effects on heat exchanger weight and performance. Early investigations into the effect of manifold pressure loss, indicated that with almost all of the promising configurations a pressure drop split of approximately 85 percent in the heat exchanger core and 15 percent in the manifolds resulted in the most satisfactory solution. As this reduction of 15 percent in the pressure drop being allowed for the heat exchanger cores causes only a slight change in dimensions and weight of the cores, no new designs were made but the pressure drop in the existing designs increased. The designs shown in the following figures have manifolds designed to utilize 15 percent of the core drop and the overall pressure drop in these designs has, therefore, been increased by 15 percent on either side.

At the low effectiveness and reasonably high pressure drop conditions, all heat exchangers derived utilizing this type of core matrix, had dimensions close to those of typical liquid to liquid tubular heat exchangers. As the computer program generates a rectangular bundle of tubes, the simplest possible packaging is to put this bundle of tubes into a rectangular box. Figure 7 illustrates how a heat exchanger with an effectiveness of 0.75 and a total pressure drop ($\Delta P/P$) of 4 percent could be packaged in this manner. A disadvantage of this type of

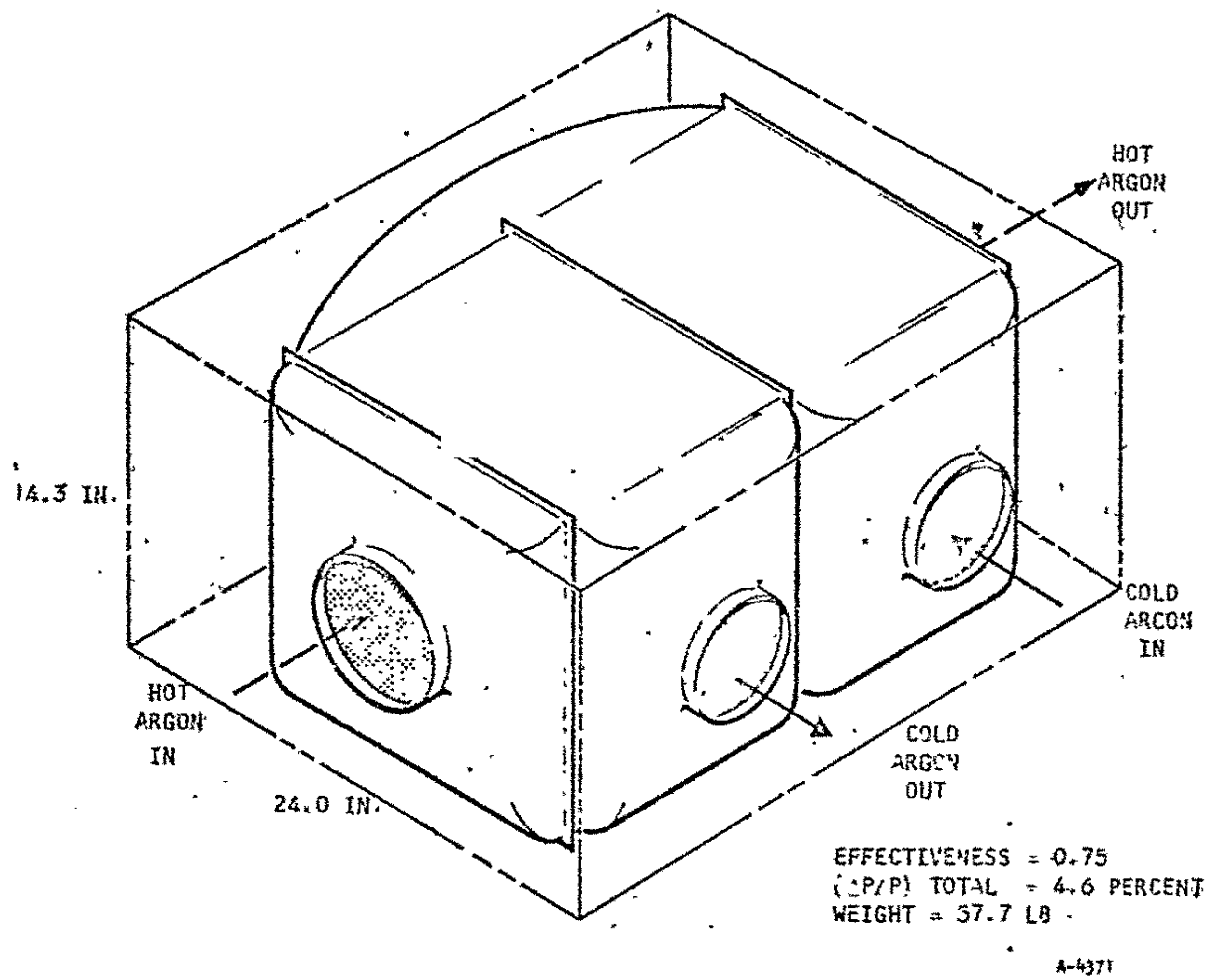

Figure 7. Simple Packaging of Tubular
Cross Counterflow Heat Exchanger

packaging is the large, flat, unsupported faces that appear on the top and bottom of the heat exchanger. These faces would either have to be built from honeycombed structure or to have supports or stiffeners provided in order to contain even the low operating pressures of the Brayton Cycle System. The preferred configuration for this simple type of rectangular tube bundle is shown in Figure 8. This configuration is identical to that of a typical liquid to liquid heat exchanger. The low pressure fluid flows through the tubes and the high pressure fluid makes two passes across the tube bundle. The design shown in Figure 8 is also for an effectiveness of 0.75 and a total pressure drop of 4 percent. The core selected in this case is of slightly different geometry from that used in Figure 7, to conform more readily to this type of packaging. It can be seen from the weights shown on the two figures that not only does Figure 8 represent a better pressure vessel, but it also yields a lighter weight solution. As effectiveness increases so does heat exchanger size and Figure 9 illustrates how a heat exchanger with an effectiveness of 0.8 would appear if packaged in the simplest possible manner. Figure 10 illustrates how a package of this type may be changed to minimize the one long dimension. In this case the tubes are merely put into two bundles side by side rather than end to end, however, as can be seen from the weights on these two figures, the reduction in maximum length is also accompanied by an increase in weight. In all the four illustrations described so far, the packaging concepts utilized have applied primarily to the best size solutions of Figure 4, 5 and 6. In all cases there are solutions available which have substantially lighter weights. The problem of packaging these minimum weight solutions requires a different technique than the very simple one illustrated thus far. The main packaging problem arises from the very large no flow lengths which accompany the tight, restrictive, transfer surfaces which yield the minimum weight solutions. By far the most attractive packaging concept for this type of heat exhanger core is the use of multiple concentric rings. A typical configuration for a heat exchanger utilizing this concept and designed for an effectiveness of 0.85 and a total pressure drop of 2.5 percent is shown in Figure 11. The core weight for this particular design was 59.0 lbs. while the final wrapped up weight as shown on the figure, was 91.3 lbs. It is of interest to note that the so-called "best size" core for these operating conditions had a core weight of 104 lbs. This weight is in excess of the total wrapped weight of the minimum weight core. As effectiveness increases and pressure drop decreases, the benefits of this particular type of packaging are increased. Even at the low effectiveness and high pressure drop conditions, the use of a single ring design, generally yields the most satisfactory solution. Figure 11A shows a typical single ring design.

This annular concept of packaging was, therefore, used for all cores of this type. From the very large number of heat exchanger cores designed by the computer program, designs were selected for effectiveness of 0.75, 0.80, 0.85 and 0.90 and for nominal pressure drops of 1.0, 2.5, 4.0, 6.0 and 8.0. The cores selected for each of these points were then packaged in the concentric ring concept discussed above and overall dimensions and weight calculated. A chart of all these results was prepared and is shown in Figure 12. As pointed out above, no redesign of the heat exchanger cores was made to allow for the 15 percent manifold pressure losses. The actual pressure losses in the heat exchangers are, therefore, a little in excess of the nominal values. A table showing both the nominal and actual pressure drops for each of the curves shown, is included on Figure 12. As in the previous figures, the actual data points

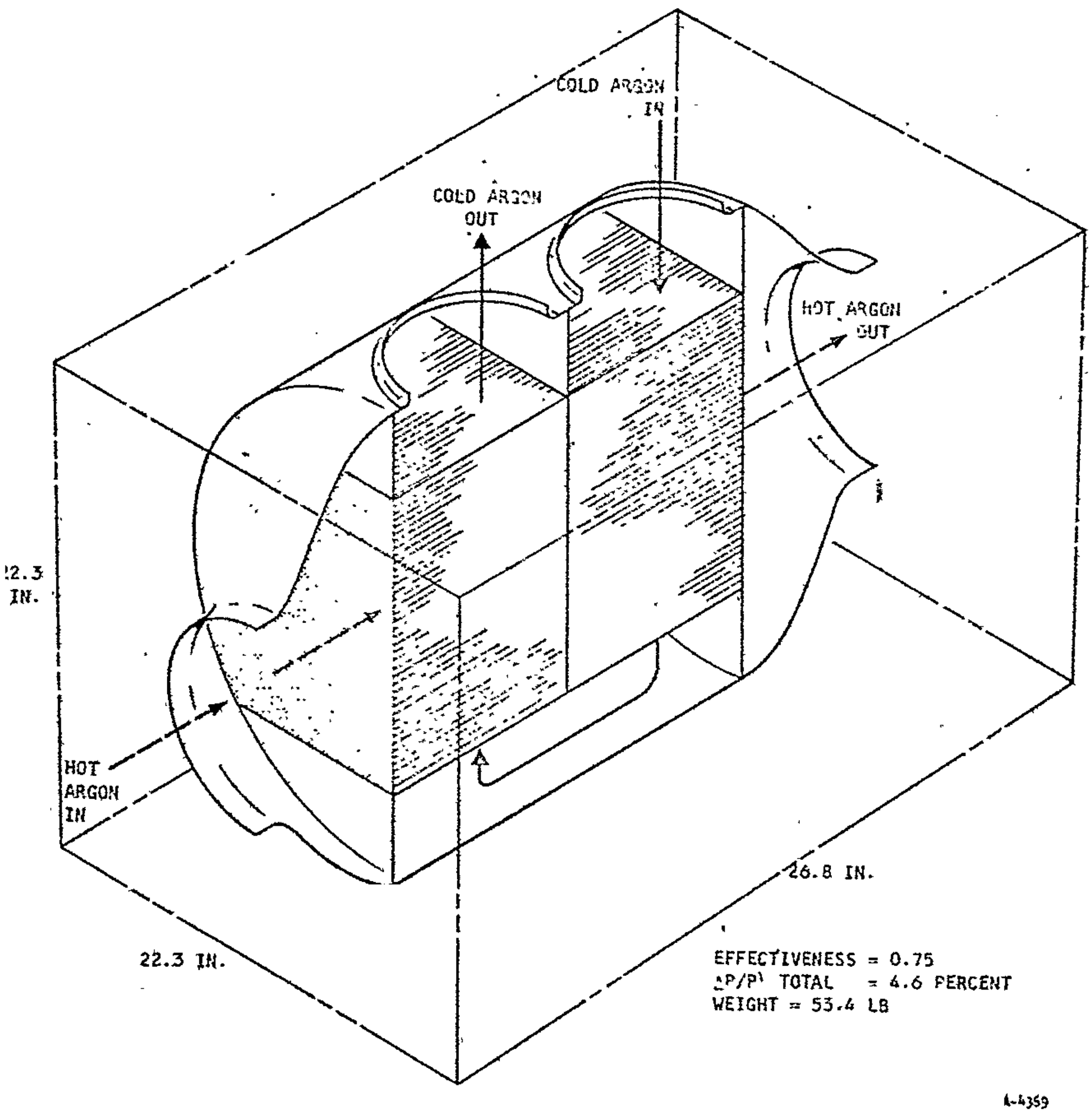

Figure 8. Conventional Packaging for Tubular Cross Counterflow Heat Exchanger

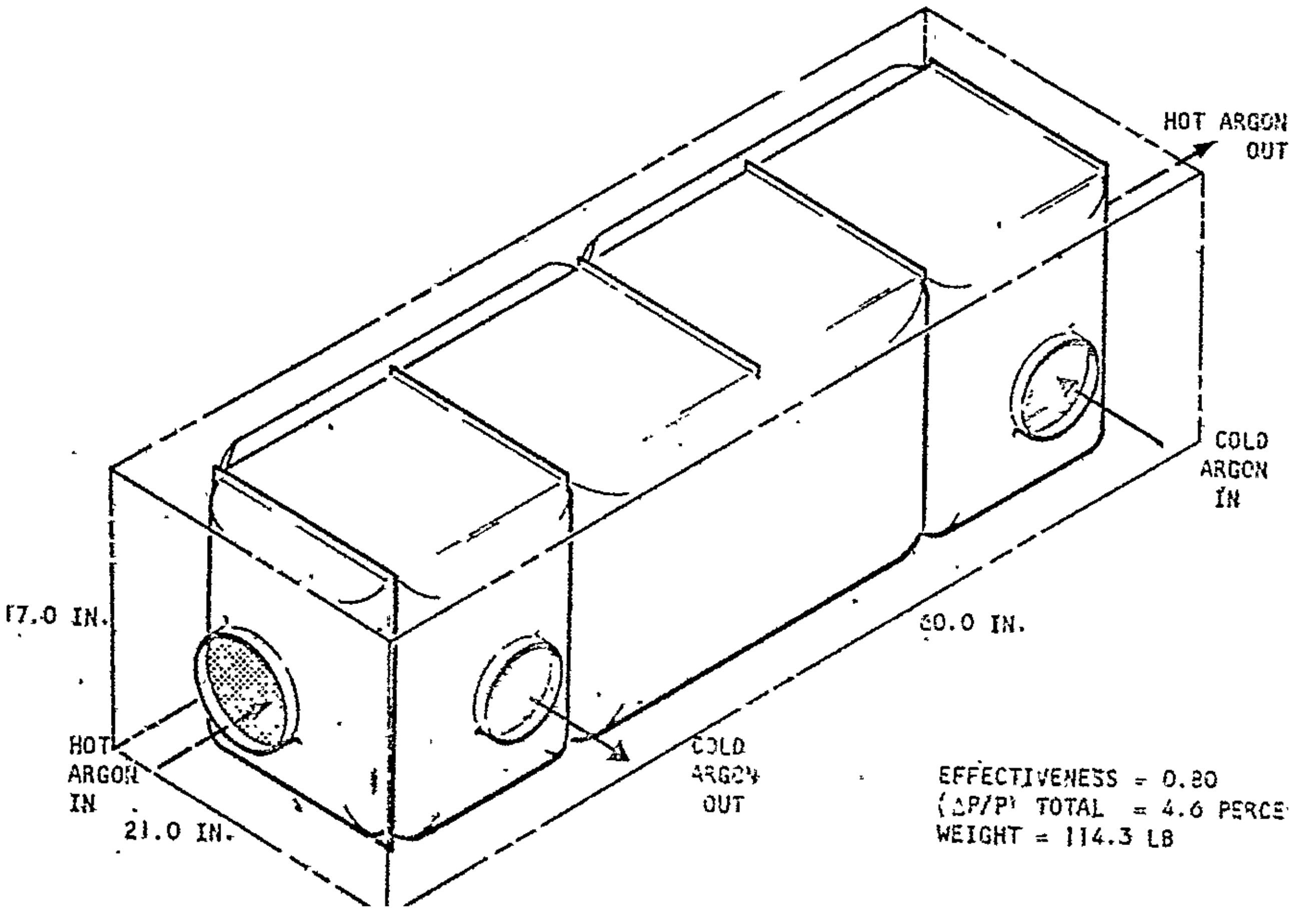

Figure 9. Typical Packaging for Tubular Cross Counterflow Heat Exchanger

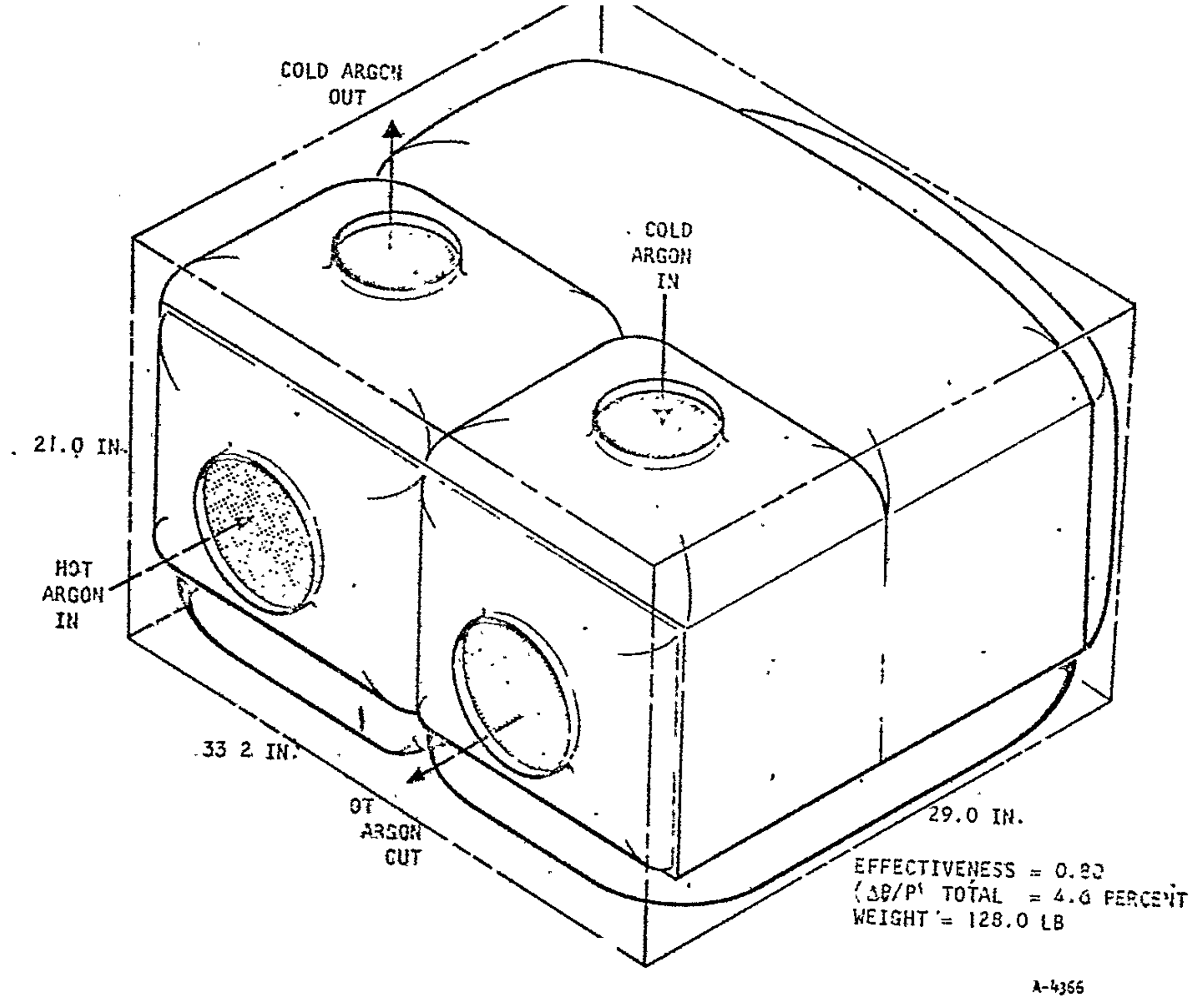

Figure 10. Alternate Packaging for Tubular Cross Counterflow Heat Exchanger

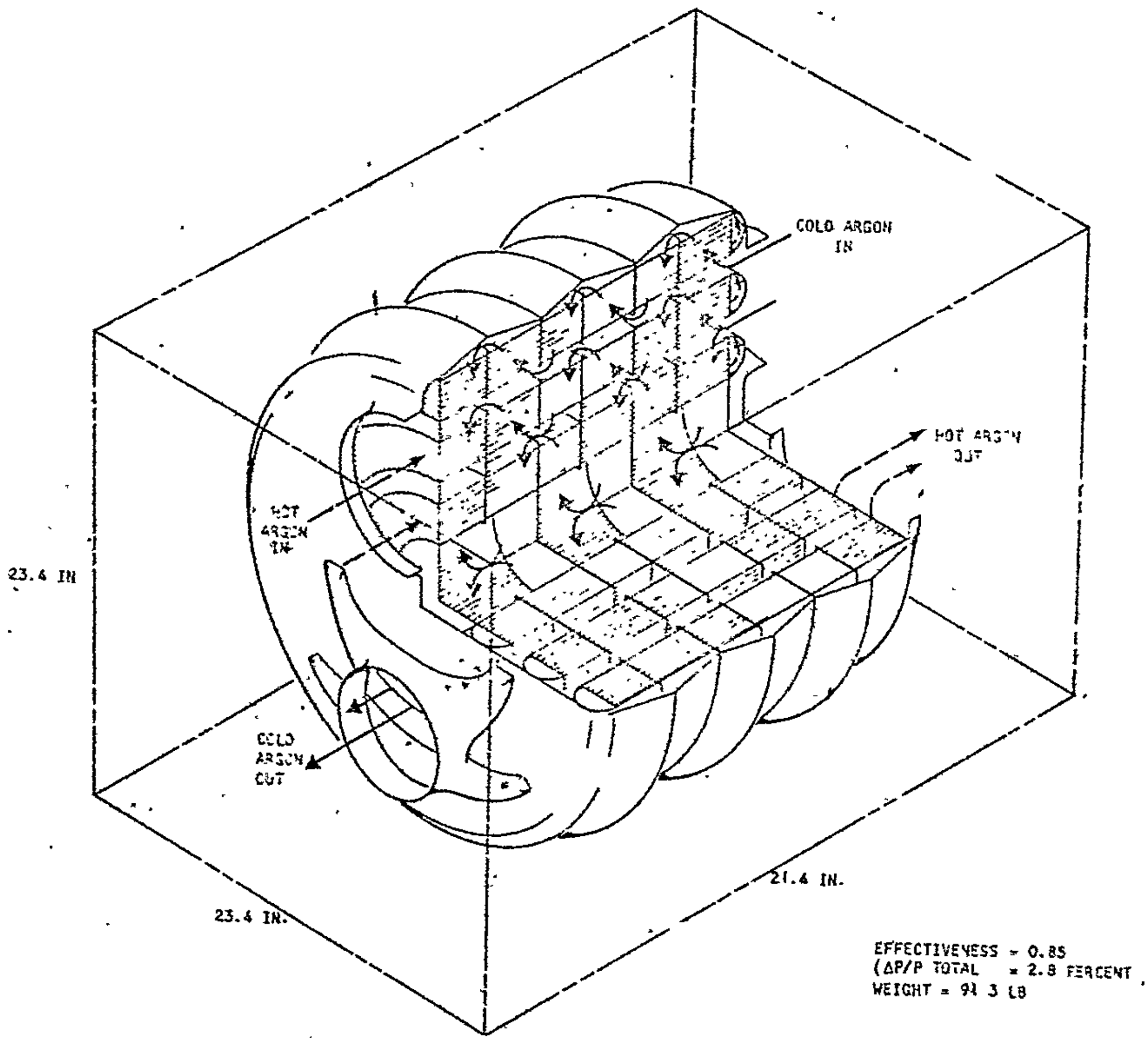

Figure 11. Multi-Concentric Ring Packaging of Tubular Cross Counterflow Heat Exchanger

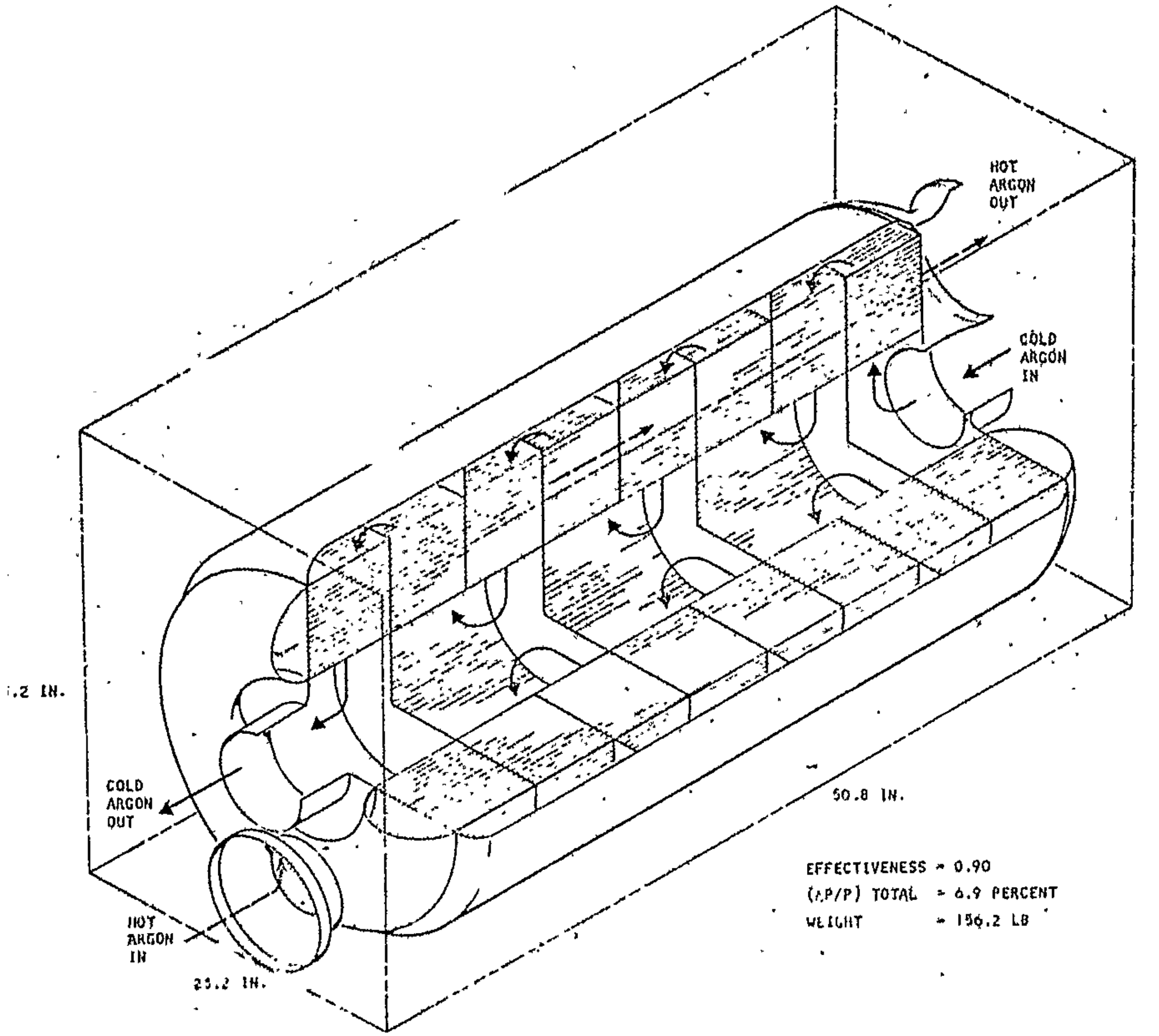

Figure 11a. Single Ring Packaging of Tubular Cross-

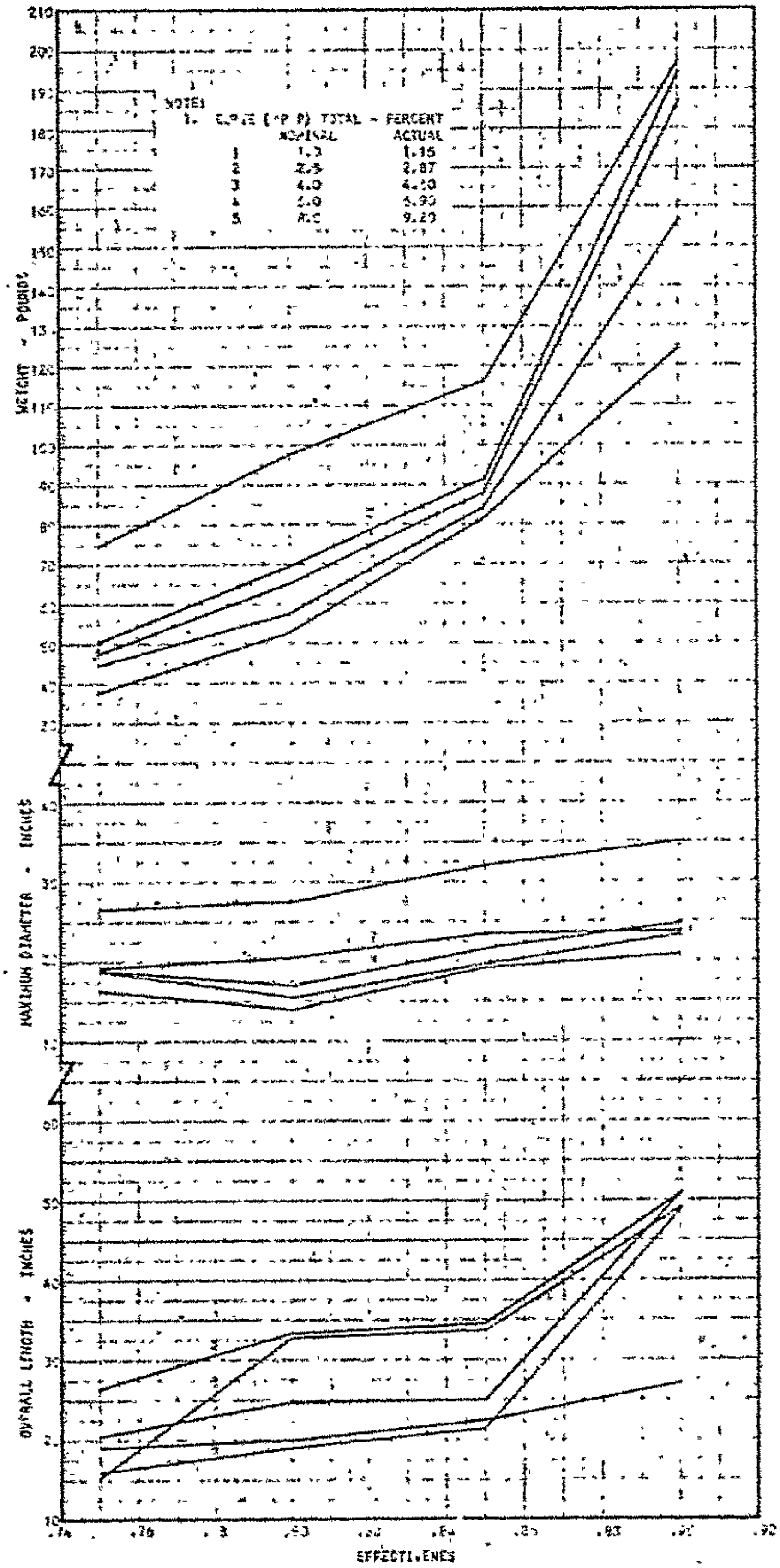

Figure 12. Tubular Multipass Cross Counterflow Heat Exchanger Parameters Versus Effectiveness

quoted are connected by a series of straight lines. Also, as before, the absence of smooth curves and easy interpolation is due to the fact that as problems conditions change, the optimum matrix geometry also changes. These curves of Figure 12 do, however, illustrate clearly the effect of both effectiveness and total pressure drop on recuperators designed utilizing the multipass, cross counterflow tubular heat exchanger design concept.

Multipass Cross-Counterflow Plate Fin Heat Exchangers

As with the multipass tubular heat exchanger solutions, a very large number of matrix geometries were considered for the full range of problem conditions. The construction of all plate and fin matrices considered in this section of the study utilized 0.004 in. thick, nickle fins and 0.006 in. thick, stainless steel plates throughout. The nickle fins are preferred to stainless steel because of the higher thermal conductivity of nickle which greatly benefits the usefulness of the extended surface. Figures 13, 14 and 15 summarize representative results obtained from the computer program used to design the plate fin multipass cross-counterflow heat exchangers. The results shown in these figures are for the heat transfer matrix only and no allowance has been made for packaging or manifolding. Also the full available pressure drop is used within the core and, as with the cross-counterflow tubular solutions, allowances have to be made for manifolding pressure losses. Figure 13 shows the weight and the three basic dimensions of the heat transfer matrix plotted against effectiveness for three different pressure drop levels. As effectiveness increases, so does the number of passes and the number of passes actually utilized at each effectiveness is shown on the figure. Figures 14 and 15 show the effect of changing total pressure drop on heat exchangers with effectiveness of 0.75 and 0.90 respectively. In all cases with this type of heat transfer matrix, even at the lowest effectiveness and highest pressure drop, the no-flow dimension of the core is very large when compared to the other two dimensions. This very long no-flow dimension introduces packaging and manifolding problems and even in the cases of the so-called best size solutions, careful attention must be paid to packaging in order to obtain reasonable overall dimensions.

Utilizing the simplest form of packaging for this type of core, that is, leaving the no-flow dimension as a single length, a core of the type illustrated in Figure 16 is evolved. This type of design is obviously unacceptable from the flow distribution standpoint as the manifold lengths are so great that a large part of the heat transfer matrix would be starved of flow. The very awkward appearance of this core is considerably emphasized by the inlets and outlets shown. The duct diameters of 8 in. on the low pressure side and 6 in. on the high pressure side were arbitrarily selected and are utilized on most figures shown in the parametric study. These duct sizes appear compatible with maintaining the very low pressure drop throughout the system. The particular heat exchanger shown in Figure 16 was designed for an effectiveness of 0.8 and a total pressure drop of 4 percent. Even at these fairly modest operating conditions and utilizing the "best size" type of solution, the overall package dimensions, using the simplest form of packaging are not acceptable. At a slightly higher pressure drop level (6 percent) and the same effectiveness and utilizing a form of packaging which divides the no-flow length into two equal portions, a somewhat improved form of packaging may be obtained as illustrated in Figure 16a. For the range of operating conditions for the solar

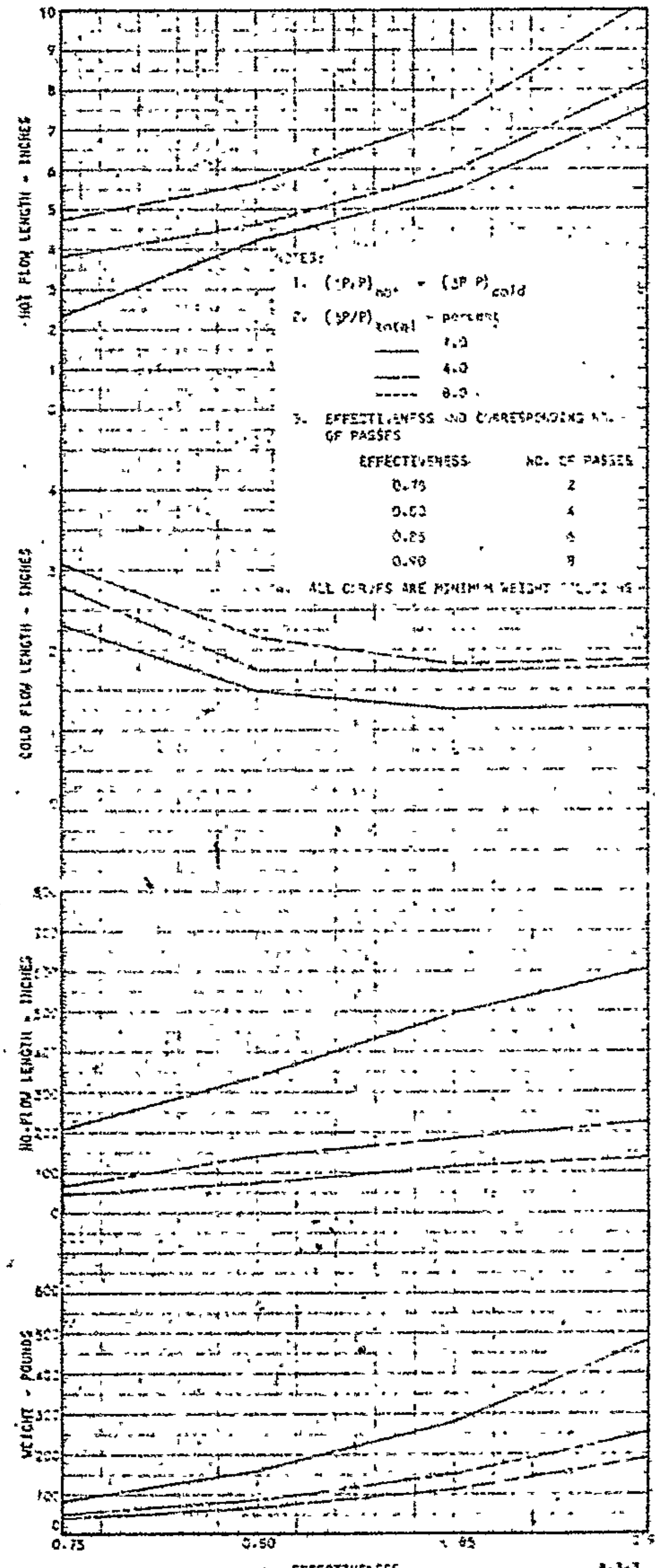

igure 13. Plate-Fin Multipass Cross Counterflow Core Parameters Versus Effectiveness

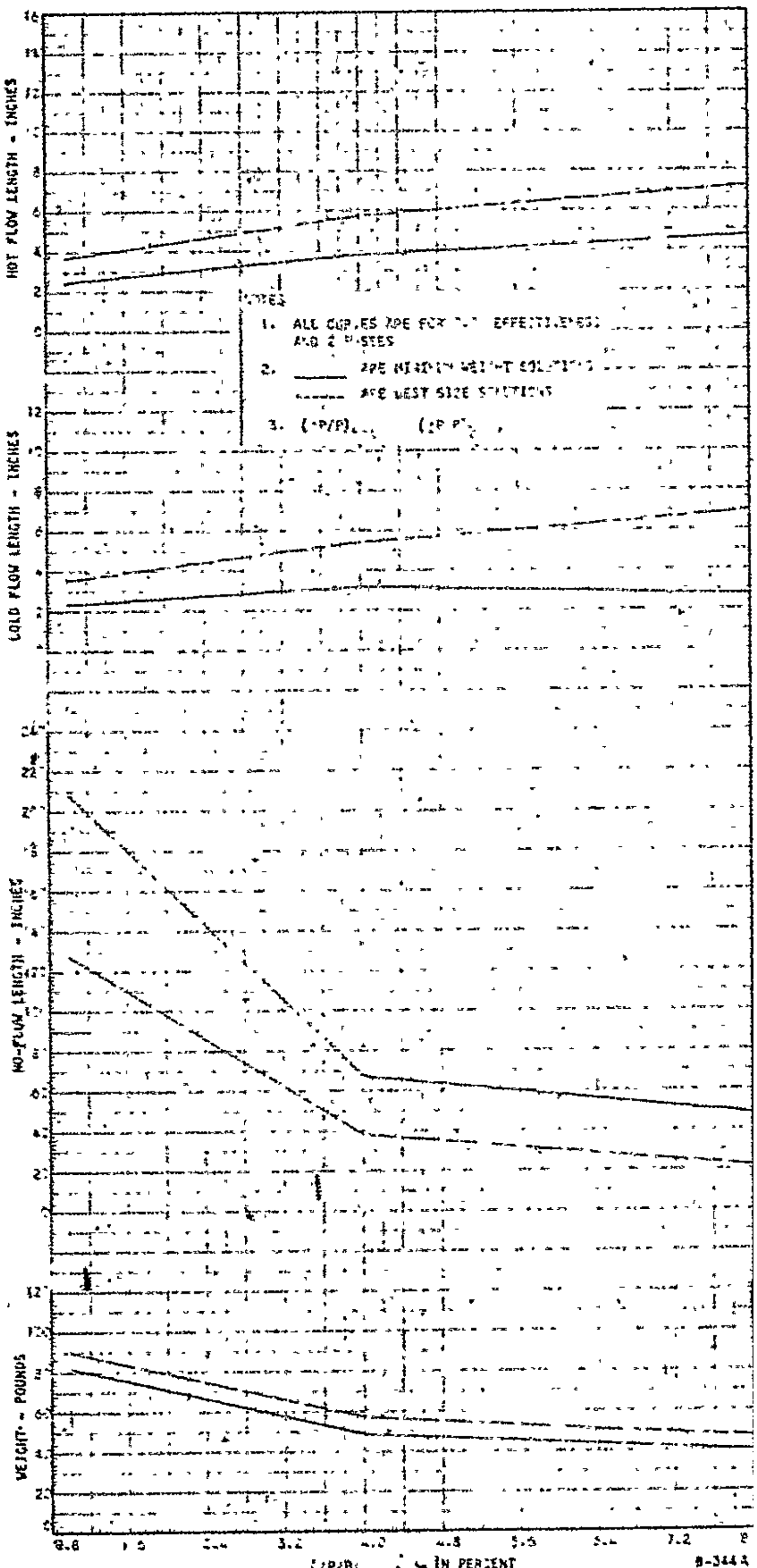

Figure 14. Plate-Fin Multipass Cross Counterflow Core Parameters Versus Percent Pressure Drop

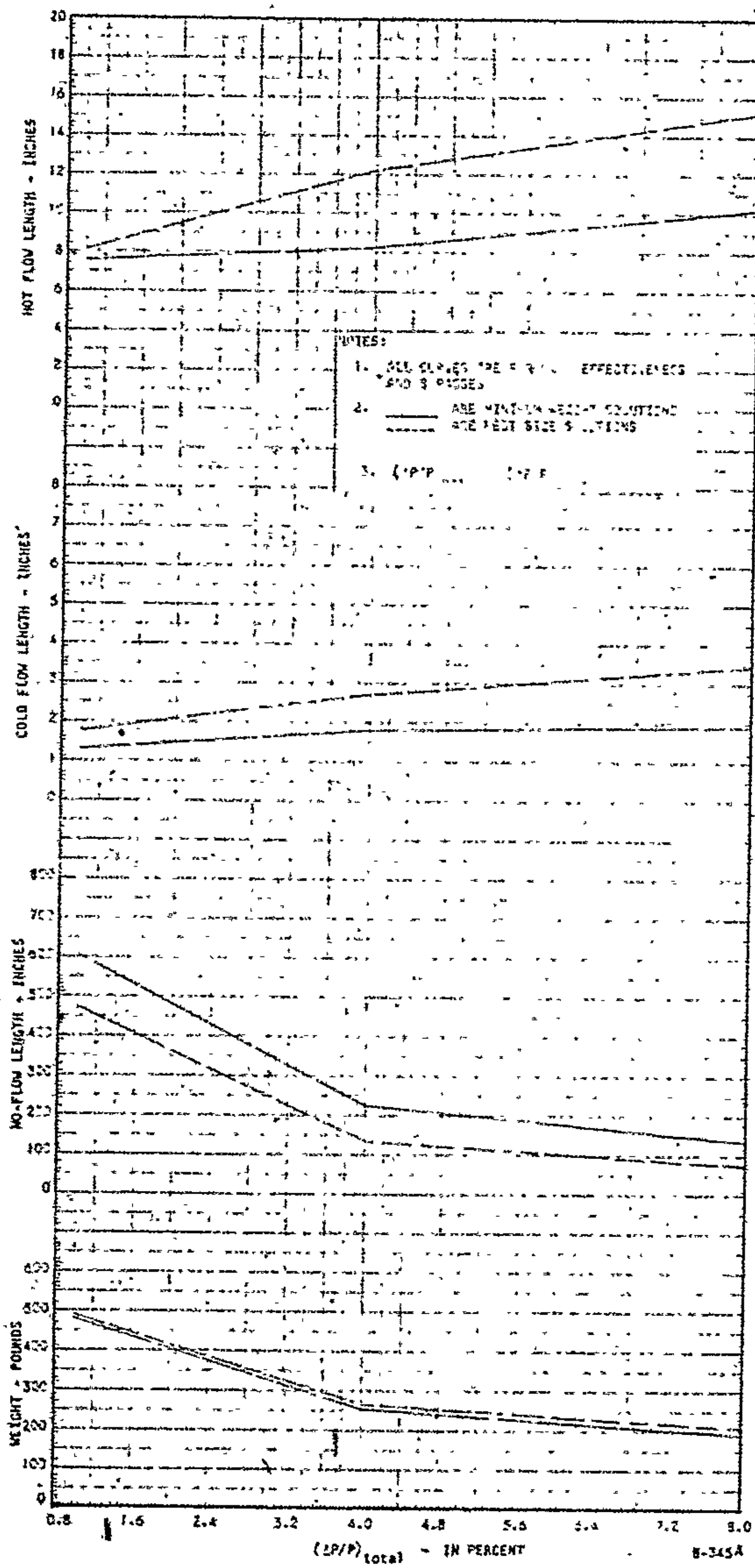

Figure 15. Plate-Fin Multipass Cross Counterflow Core Parameters Versus Percent Pressure Drop

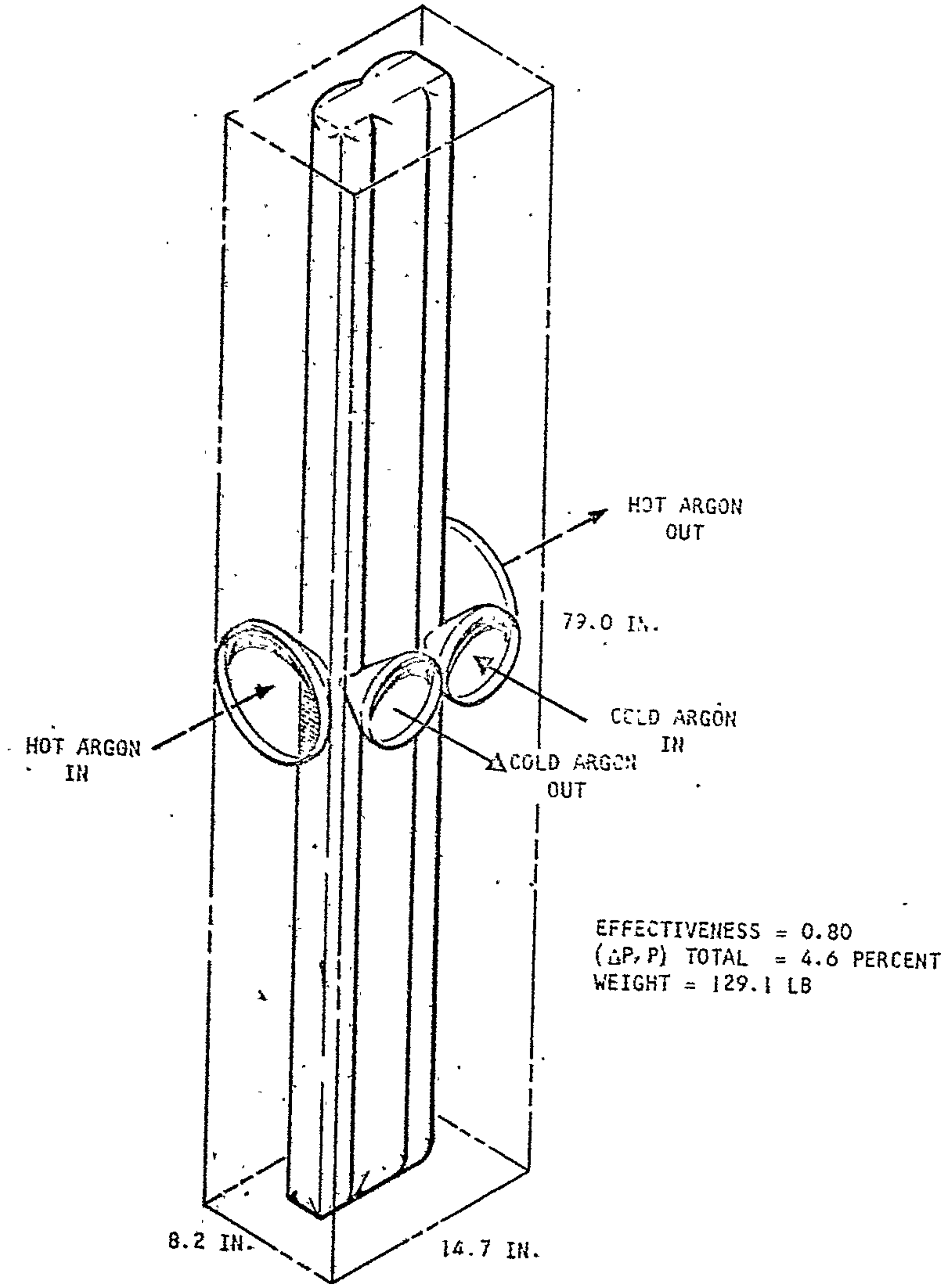

Figure 16. Simple Packaging of Plate-Fin Cross Counterflow Heat Exchanger

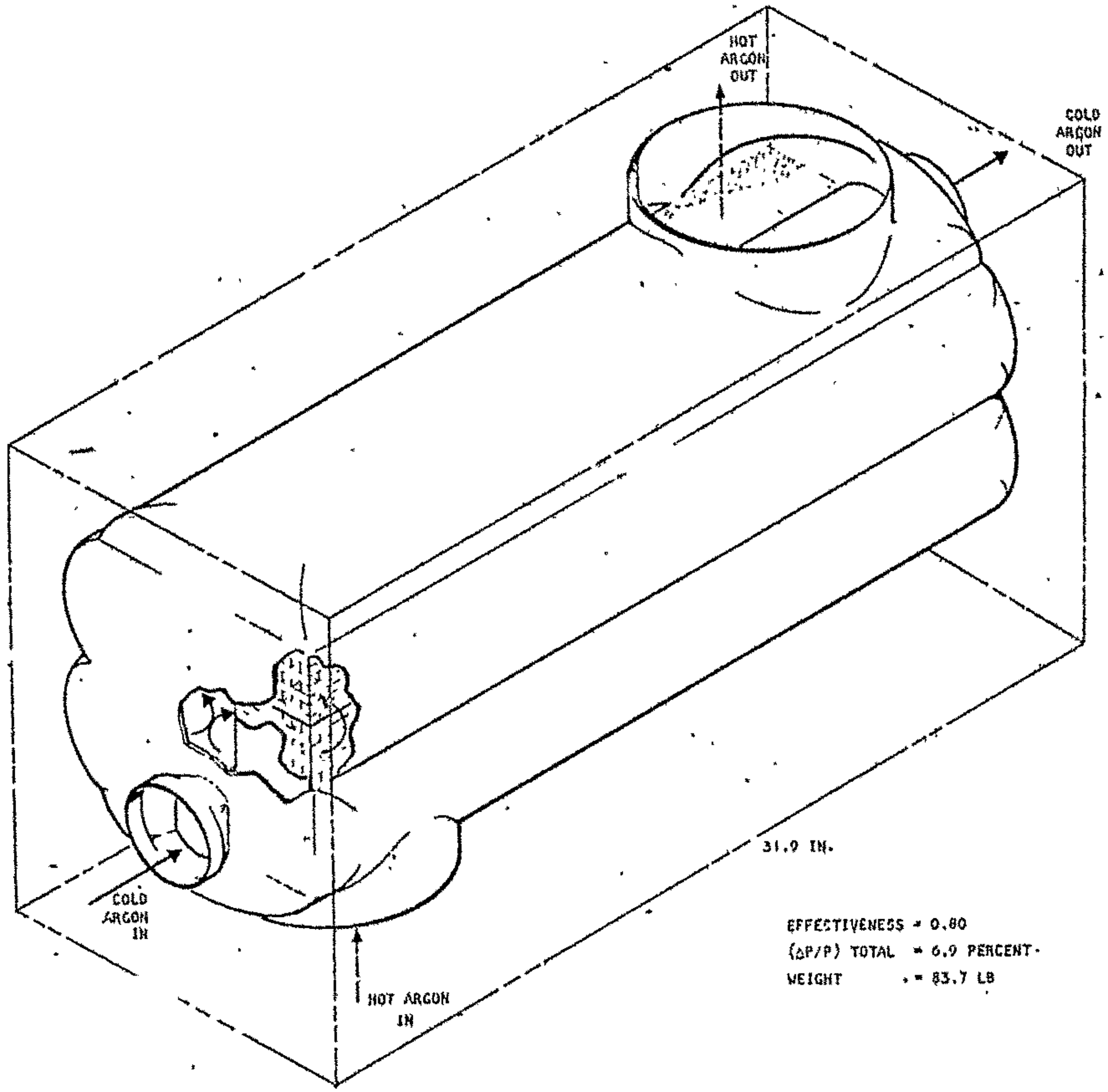

Figure 16a. Typical Plate-Fin Cross Counterflow Heat Exchanger

powered Brayton cycle recuperator, no plate fin matrix was found which resulted in a solution which gave both acceptable weight and simple packaging.

A comparison of Figures 13, 14 and 15 with Figure 12 plainly shows that over the entire range of operating conditions, not only are the plate and fin cores somewhat heavier than the wrapped-up tubular cores, but also the complexities of packaging the plate and fin cores would not yield as attractive packages as the tubular heat exchangers. There is, therefore, no point in the operating conditions of the solar Brayton cycle recuperator where a multipass plate and fin heat exchanger yields a optimum solution. Owing to this fact, no further packaging concepts were prepared and no curves showing overall dimensions and weight of fully packaged plate and fin heat exchangers are presented.

Pure Counterflow Tubular Heat Exchangers

When the contract to conduct this parametric survey was received from NASA, AiResearch did not have the computer program to design pure counterflow tubular heat exchangers. As part of this contract, a program was written and has been described earlier in this report. The main limitation to the use of this program and to the design of this type of heat exchanger, is the lack of reliable heat transfer and friction factor data for flow outside and parallel to, tube bundles. This lack of data and the search conducted by AiResearch into the data that is available, has also been previously discussed in this report. In order to determine whether or not this type of matrix was suitable for any part of the range of operating conditions being studied, it was necessary to assume some predictable operating conditions for the flow outside the tubes. All preliminary investigations of this type of matrix, therefore, used the Colburn Modulus and Fanning friction factor data for flow inside plain round tubes. As with the cross-counterflow tubular heat exchanger designs, all stainless steel construction was used throughout and a wall thickness of 0.004 in. was maintained. By varying tube diameter and tube spacing, a large number of matrix geometries were examined for each problem condition. The results obtained from these preliminary computer runs are shown in Figures 17 and 18. In this particular type of heat transfer matrix, there are only two overall package dimensions. These two dimensions are face area (or number of tubes) and tube length. There is no theoretical limitation in the way the face area is arranged and throughout the study all computer results were obtained as a rectangular tube bundle with the face aspect ratio of 1.0. The face dimension shown in Figures 17 and 18 is, therefore, one side of a square face. Also shown in Figures 17 and 18 are small tables showing both the nominal and actual pressure drop of each of the curves appearing on these figures. The nominal pressure drops shown represent the actual input conditions fed into the computer, while the actual pressure drops shown represent the total pressure drop utilized in the final design. The difference between the nominal and actual pressure drop results from the fact that only one side of these pure counterflow heat exchangers utilizes the full available pressure drop and the other side utilizes only a fraction of the given input. The program is so written that the side requiring the most pressure drop is always controlling and therefore, the total pressure drop for any design is always less than the nominal.

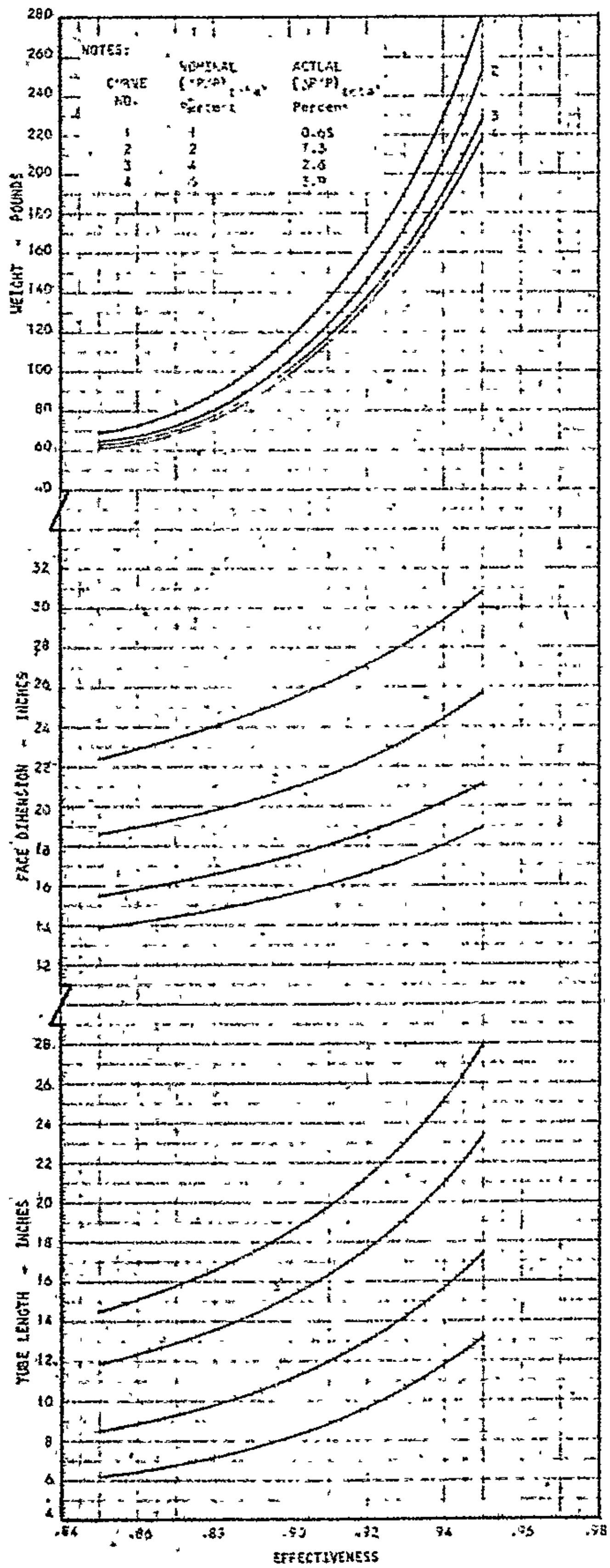

Figure 17. Tubular Pure Counterflow Minimum Weight Cores Versus Effectiveness

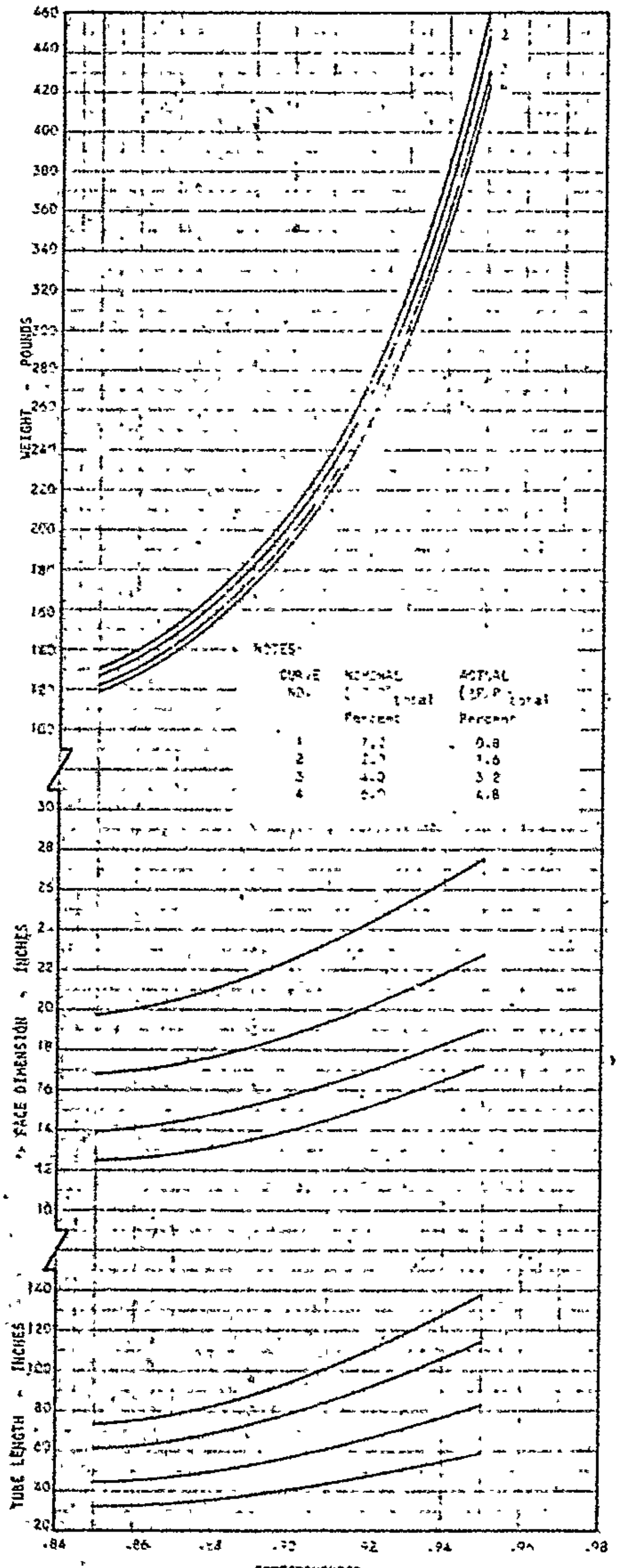

Figure 18. Tubular Pure Counterflow Minimum Face Area Cores Versus Effectiveness

Figure 17 presents a summary of the minimum weight solutions obtained for the range of operating conditions examined. The range of conditions examined for this type of heat exchanger, was limited to effectivenesses greater than 0.85 and nominal pressure drops of less than 6 percent. From the figure it can be seen that weight increases rapidly with increasing effectiveness while both face area and tube length increase at a somewhat slower rate. The influence of overall pressure drop on heat exchanger weight is not great, but its influence on package dimensions is pronounced. As pressure drop is decreased, face area increases and tube length decreases. In all the designs utilized to prepare Figure 17, no allowance is made to either dimensions or weight for manifolding and packaging. All designs do, however, consider the effect of axial conduction. The method of allowing for the effect of axial conduction in this type of heat exchanger, has been previously described in this report. It is of interest to note, that at the low end of the range considered (effectiveness 0.85, ($\Delta P/P$) = 3.9 percent) the effect of axial conduction increases heat exchanger size by approximately 3 percent. At the high end of the operating range (effectiveness 0.95, ($\Delta P/P$ = 0.65 percent) the effect of axial conduction on heat exchanger size increases to 53 percent.

In order to determine what effect variations in outside tube characteristics would have on heat exchanger performance some designs where prepared using hypothetical values for both heat transfer characteristics and friction factor. The changes selected in these characteristics were purely arbitrary but, were sufficiently large to ensure that appreciable changes in core size and weight would occur. The designs presented in Figures 17 and 18 utilized the Colburn modulus and Fanning friction factor for flow in plain round tubes. The arbitrary changes selected were to increase the friction factor by 25 percent with a corresponding increase in Colburn modulus of 10 percent and to decrease the friction factor by 25 percent with a decrease in Colburn modulus of 10 percent. The effect of these arbitrarily selected changes in outside the tube bundle characteristics on heat exchanger size is clearly shown in Figure 19. At all effectivenesses from 0.85 to 0.95, the effect on heat exchanger weight is very small while the effect on heat exchanger dimensions is somewhat greater. The curves shown in Figure 19 are all for a cold pressure drop (outside tubes) of 1 percent. If a higher nominal pressure drop core is considered the changes in heat exchanger weight and size are somewhat less while if a lower pressure drop design is considered the effects are slightly greater. The main purpose in preparing Figure 19 was to show, that although the data available for flow outside and parallel to tube bundles is very vague the use of flow inside plain round tubes does not invalidate a comparison of pure counterflow tubular heat exchangers with pure counterflow and plate-fin heat exchangers. If, however, it is decided to fabricate a pure counterflow tubular heat exchanger more accurate data would be required in order to obtain an accurate determination of the dimensions required.

As with the cross-counterflow tubular solution, considerable attention must be devoted to the manifolding and packaging concepts in order to determine optimum heat exchanger configuration. As stated above, the computer program generates a tube bundle with a square face area. While this type of face area presents a very simple set of core dimensions, it is almost impossible to introduce the outside flow to the center of the bundle. In order to ensure

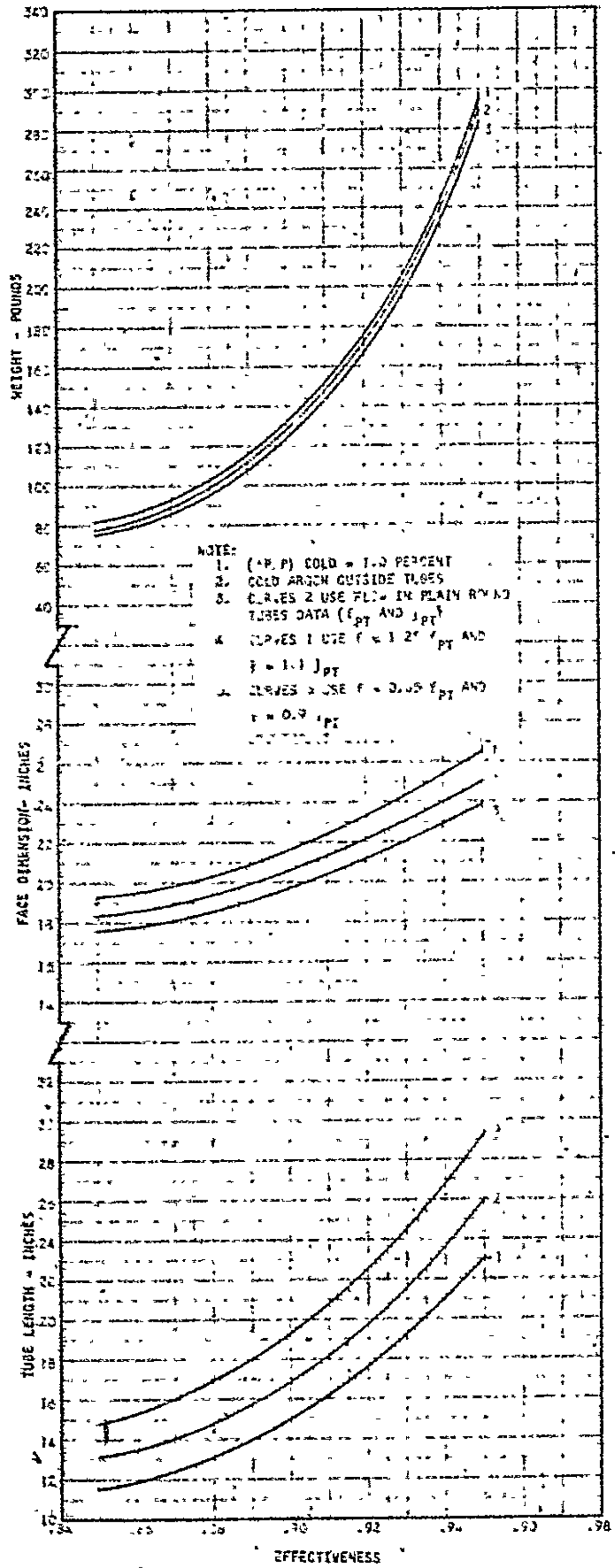

Figure 19. Effect of Outside Tube Performance Characteristics on Pure Counterflow Tubular Cores

satisfactory performance of cores of this type it is necessary to be sure that the flow on the outside the tubes' side of the bundle is actually parallel to the tubes rather than across them. It is, therefore, necessary to have one small dimension in the face area which minimizes the length across the tubes over which the flow must pass. By introducing this limitation the other dimension of the face area consequently becomes large and the same packaging problem exists as existed with the cross-counterflow tubular designs. Two different methods of packaging this type of heat exchanger core are illustrated in Figures 20 and 21. Figure 20 shows how the one long dimension of the face area may be divided into several shorter straight lengths. A means of introducing both the hot and cold fluids to this type of overall configuration is also illustrated in Figure 20. As a direct comparison to the heat exchanger shown in Figure 20, Figure 21 illustrates the identical core wrapped up in the same type of multi-concentric ring design as utilized for the cross-counterflow tubular heat exchangers. Again, Figure 21 illustrates how the fluid would be introduced to both inside and outside the tube bundle. The square design of Figure 20 has the limitation that it is not a good pressure vessel as it possesses a number of large flat faces. This design could be utilized by using honeycomb panels or some form of stiffening structure but is definitely less desirable than the concept shown in Figure 21. In addition to being a better pressure vessel, the multi-concentric ring design also has a slightly lighter weight.

Having selected the multi-concentric ring packaging concept as most suitable for this type of flow configuration, heat exchanger designs were generated covering the desired range of operating conditions. As the severity of the problem conditions being considered increases and the heat exchanger size increases more and more rings are required. In Figure 22, which illustrates the effect of pressure drop level and effectiveness on heat exchanger weight and size, the number of rings utilized varies from 3 to 6. As with the previous curves presented for heat exchanger core dimensions and weight, the small table on Figure 22 shows the nominal pressure drops which were used in the design, together with the actual overall total pressure drops.

<u>Pure Counterflow Plate Fin Heat Exchanger</u>

The matrices were assumed to be constructed of stainless steel and to utilize nickel fins 0.004 inches thick and plates 0.006 inches thick. The ratio of face area height to face area width is arbitrary for this type of heat exchanger and a ratio of 1.0 was utilized throughout the calculations.

As a preliminary step a series of designs was run off on AiResearch's IBM 7074 computer using the existing design program for this type of heat exchanger. The results from these runs are plotted in Figures 23, 24 and 25. Figure 24 shows the minimum core weight solutions, and the corresponding core dimensions as a function of effectiveness for several total $\Delta P/P$ ratios. The nominal total $\Delta P/P$ ratios represent the total pressure drops that were given as input to the computer program. Each side of the heat exchanger was allotted one half of the given total $\Delta P/P$. However, since only one side of the heat exchanger used up its allotted pressure drop, the actual total pressure drop for the designed core was less than the given nominal total pressure drop.

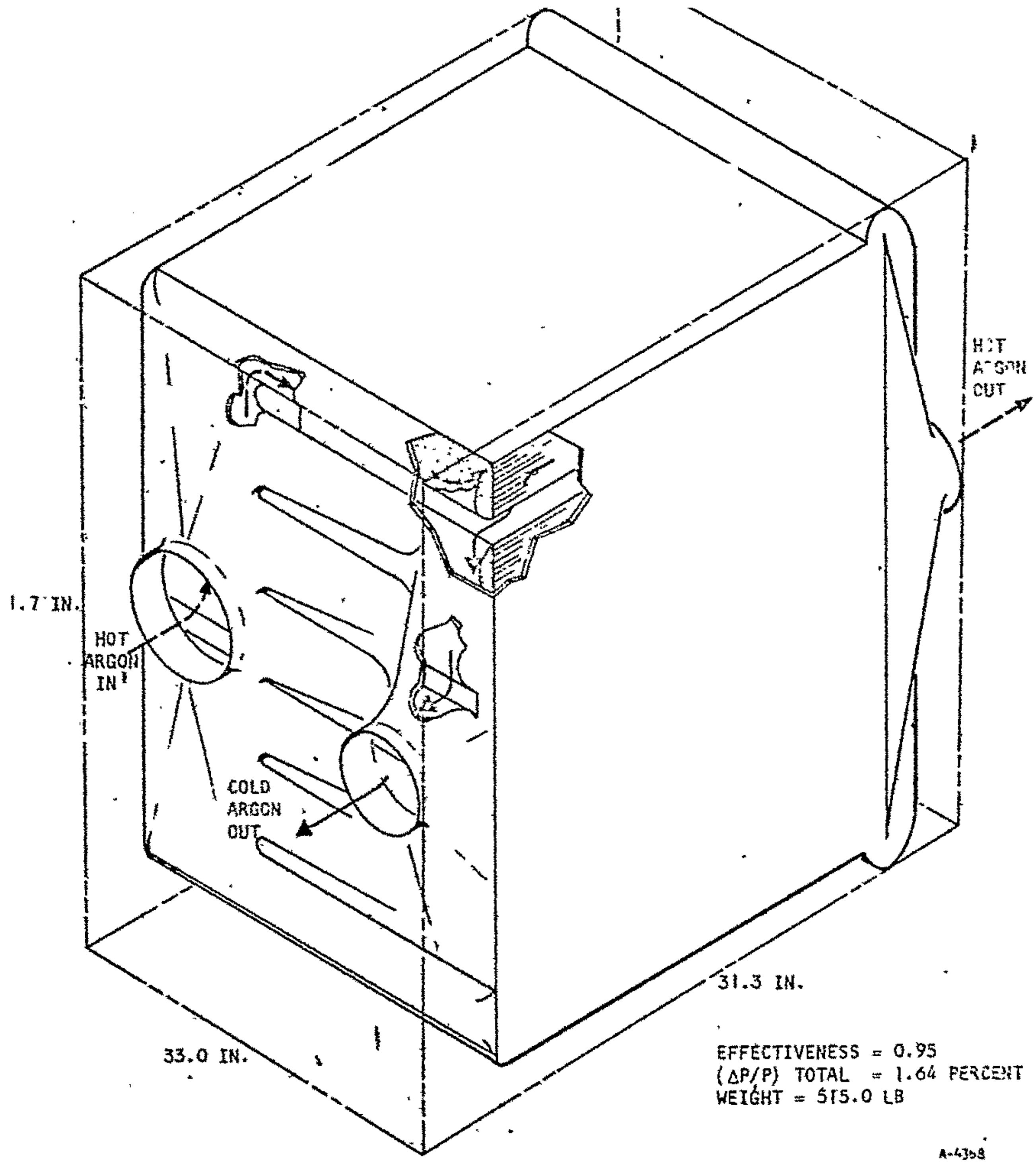

Figure 20. Rectangular Packaging of Tublar Pure
Counterflow Heat Exchanger

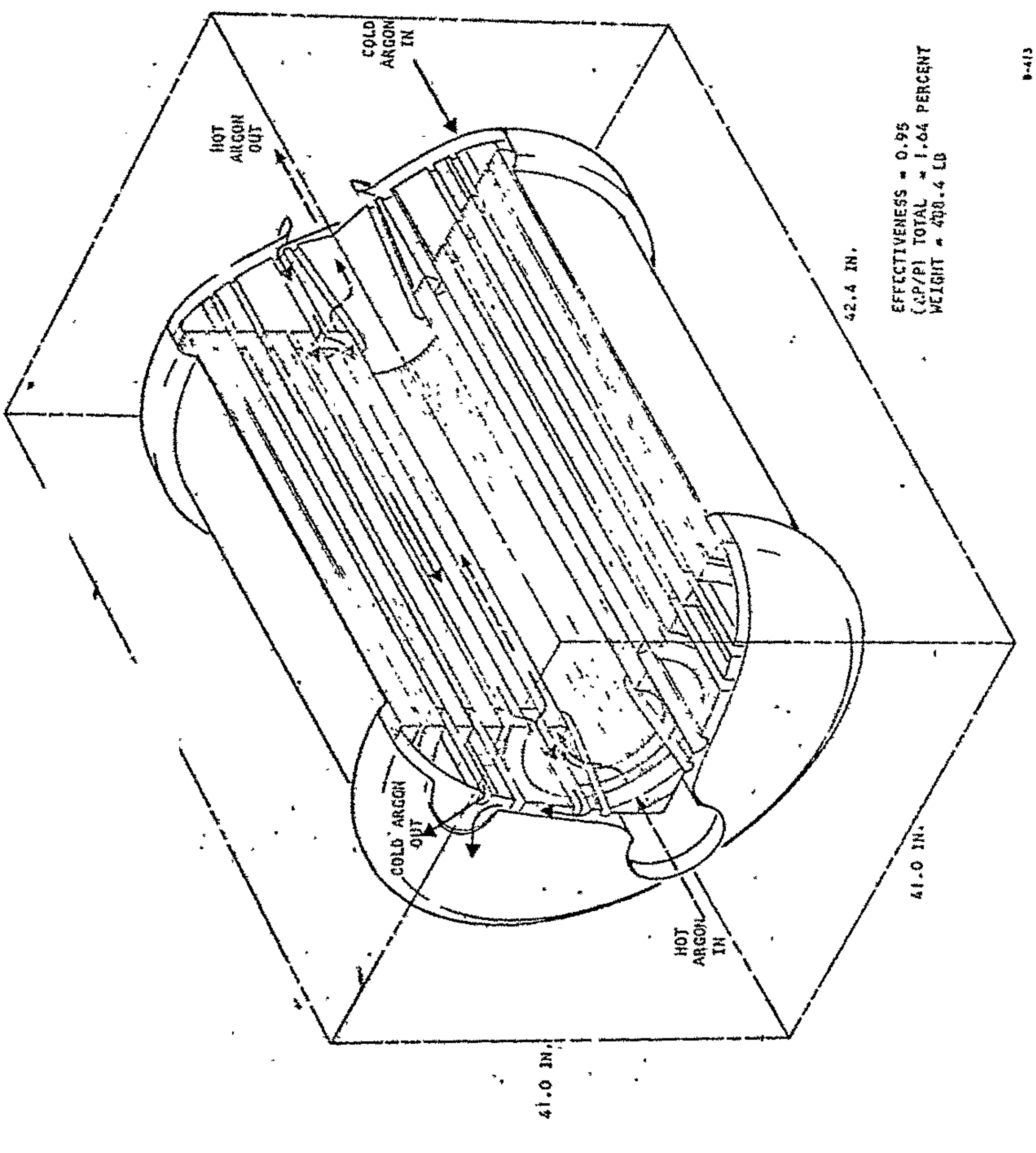

Figure 21. Multi-Concentric Ring Packaging of Tubular Pure Counterflow Heat Exchange

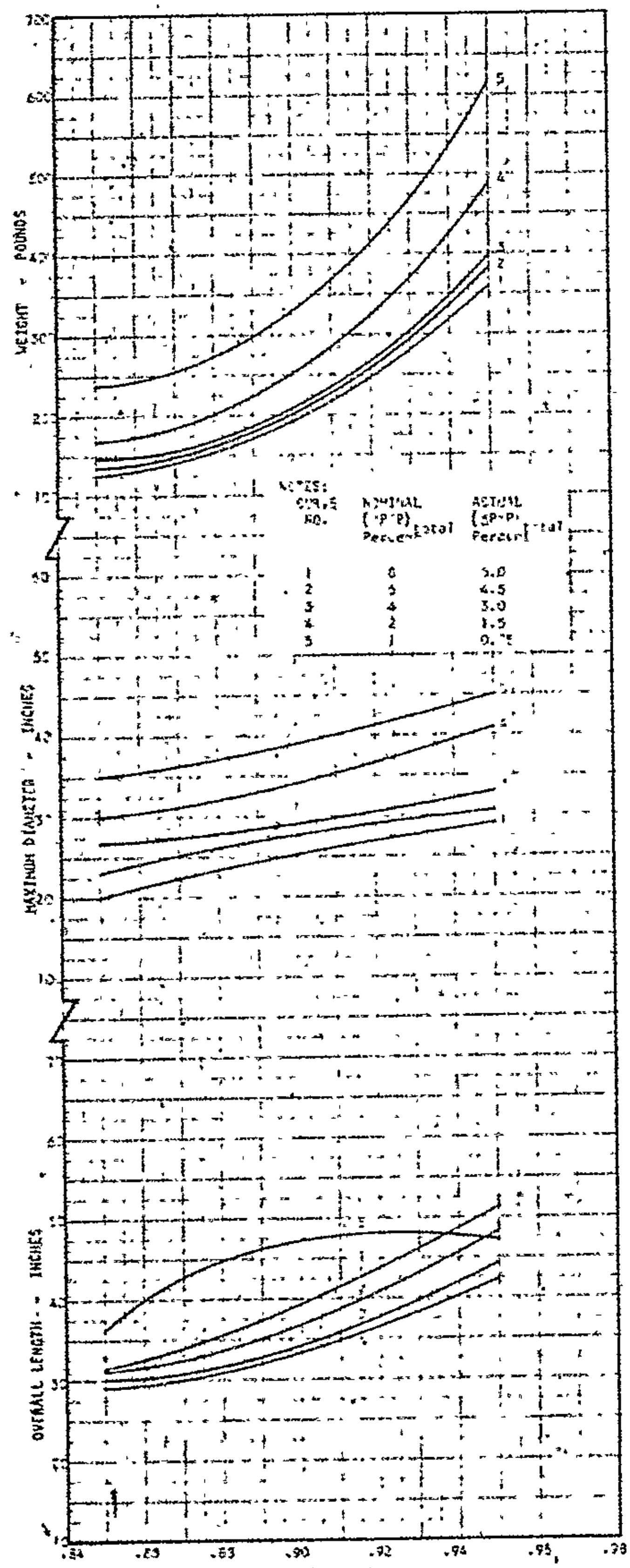

Figure 22. Tubular Pure Counterflow Heat Exchanger Parameters Versus Effectiveness

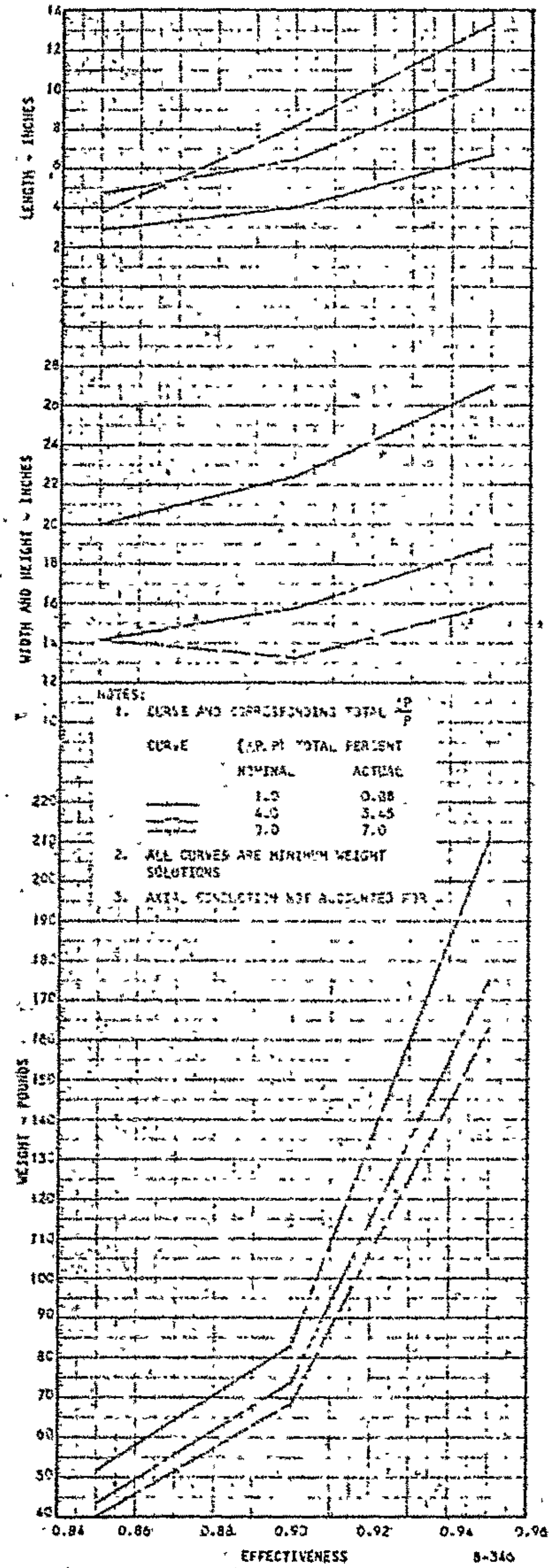

igure 23. Plate-Fin Pure Counterflow Core Parameters Versus Effectiveness

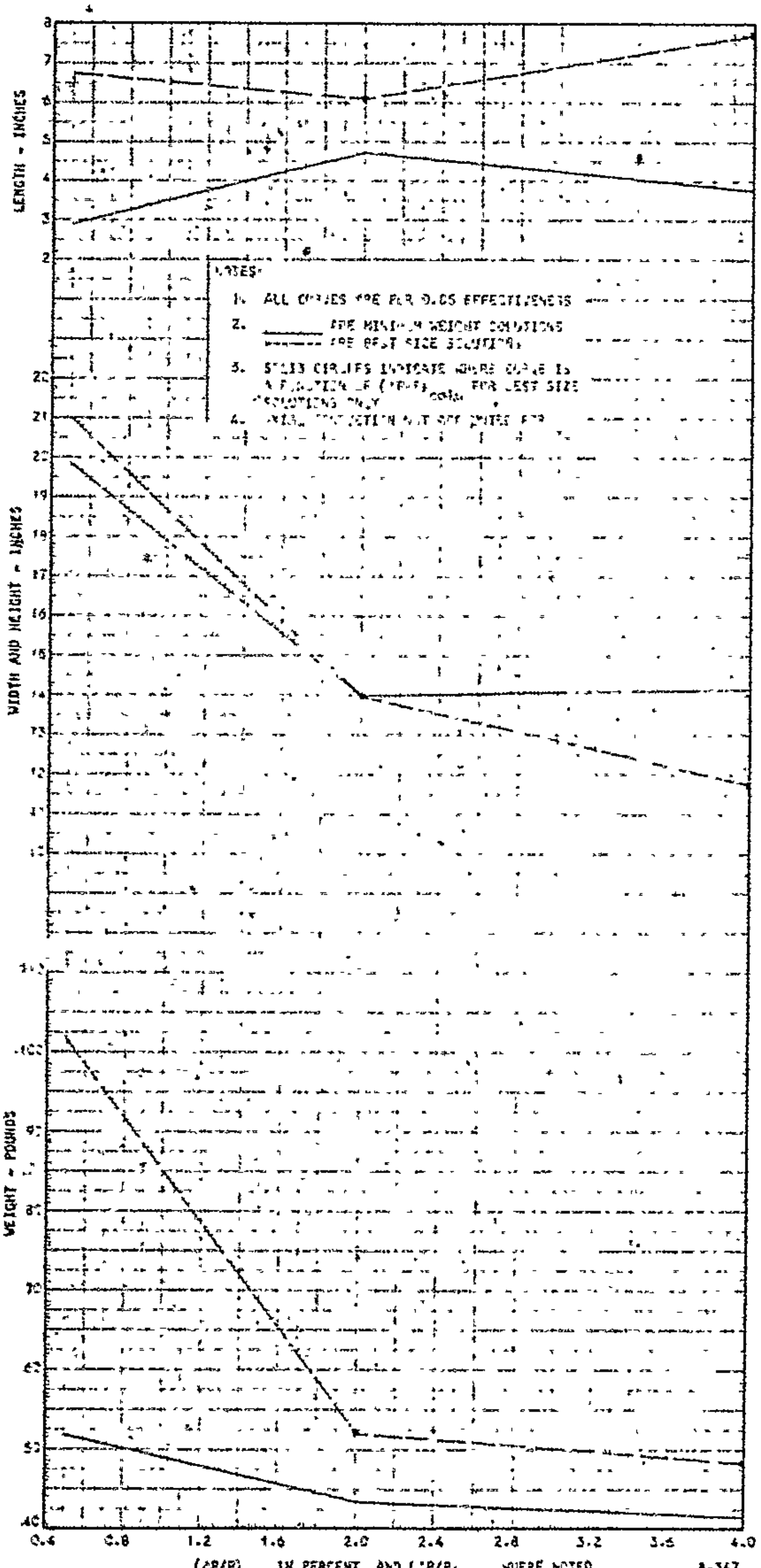

Figure 24. Plate-Fin Pure Counterflow Core Parameters Versus Percent Pressure Drop

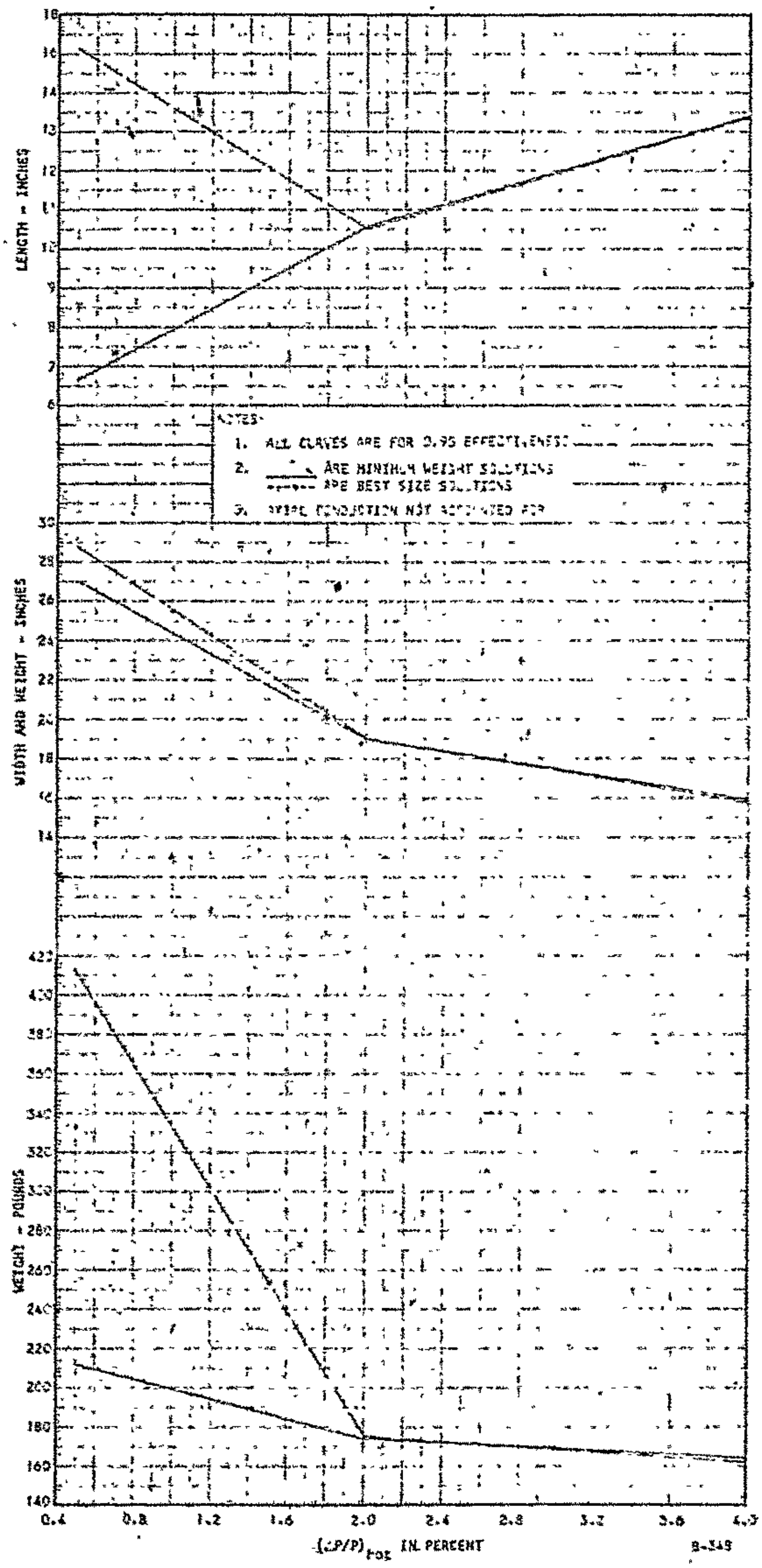

Figure 25. Plate-Fin Pure Counterflow Core Parameters Versus Percent Pressure Drop

The curves show similar trends as for the previous types of heat exchangers, that is, a large increase in both core weight and core face dimensions occurs at high effectiveness and low total $\Delta P/P$ ratios.

The effect of varying $\Delta P/P$ is shown in Figures 24 and 25. The heat exchanger parameters are plotted against percent pressure drop of the side which used up its alloted pressure drop, that is, one half of the given nominal total pressure drop. From these figures it is seen that the core weight and core face dimensions are decreased with increasing $(\Delta P/P)_{hot}$ or $(\Delta P/P)_{cold}$ as the case may be. Generally, at low $(\Delta P/P)_{hot}$ ratios the flow lengths are small and the face areas are large. This is undesirable from the standpoint of axial heat conduction and also required manifold weights. As a result, before packaging and manifolding any of these designed cores, the heat exchanger design program was modified to include the effect of axial conduction and the above cores were recalculated. The effect of axial conduction was calculated according to the simplified equations presented in another section of this report.

Two types of manifolding and packaging concepts were developed for the plate-fin pure counterflow heat exchanger. These are shown in Figures 26 and 27. The principal difference between the two is the way the hot and cold fluids are introduced to and removed from the core. The transition sections in Figure 26 are formed by single triangular plate-fin sections while those of Figure 27 are formed from double triangular sections. The entrance and exit free flow areas on both sides of both concepts are identical, but weight savings are obtained in the double triangular concept as less area and mass is used in the transition. The reduction in surface area of the transition sections in the Figure 27 concept over the Figure 26 concept does not affect the heat exchanger performance as the slight additional heat transfer that occurs in these sections is not considered in the design. In both designs the inlet and outlet triangular transition sections are of a plate-fin construction with low density fins on the cold or high pressure side only. The weight of the packaged heat exchanger tends to be less when the fluids are introduced in the manner of Figure 27 as compared to Figure 26, but the double triangular concept of Figure 27 yields a longer overall length. Therefore, the computer designed cores for the rest of the problem statement range were all packaged and manifolded as shown in Figure 27. The weights and dimensions of these packaged cores are plotted in Figure 28 against effectiveness. Several curves are shown each for a different overall total $\Delta P/P$ ratio. These ratios are actual figures and include, besides core pressure drop, the pressure drop due to the inlet and outlet manifolds and transition sections.

COMPARISON AND SUMMARY OF HEAT EXCHANGER TYPES

The foregoing discussion has outlined the complete investigations conducted on the four types of heat transfer matrices being considered. Several important conclusions have been drawn regarding each of the types considered. In all cases it was determined that a pressure drop split of approximately 85 percent in the core and 15 percent in the manifolds resulted in the most suitable design. Most suitable design may be defined as that design which yielded minimum weight or close to minimum weight heat exchanger

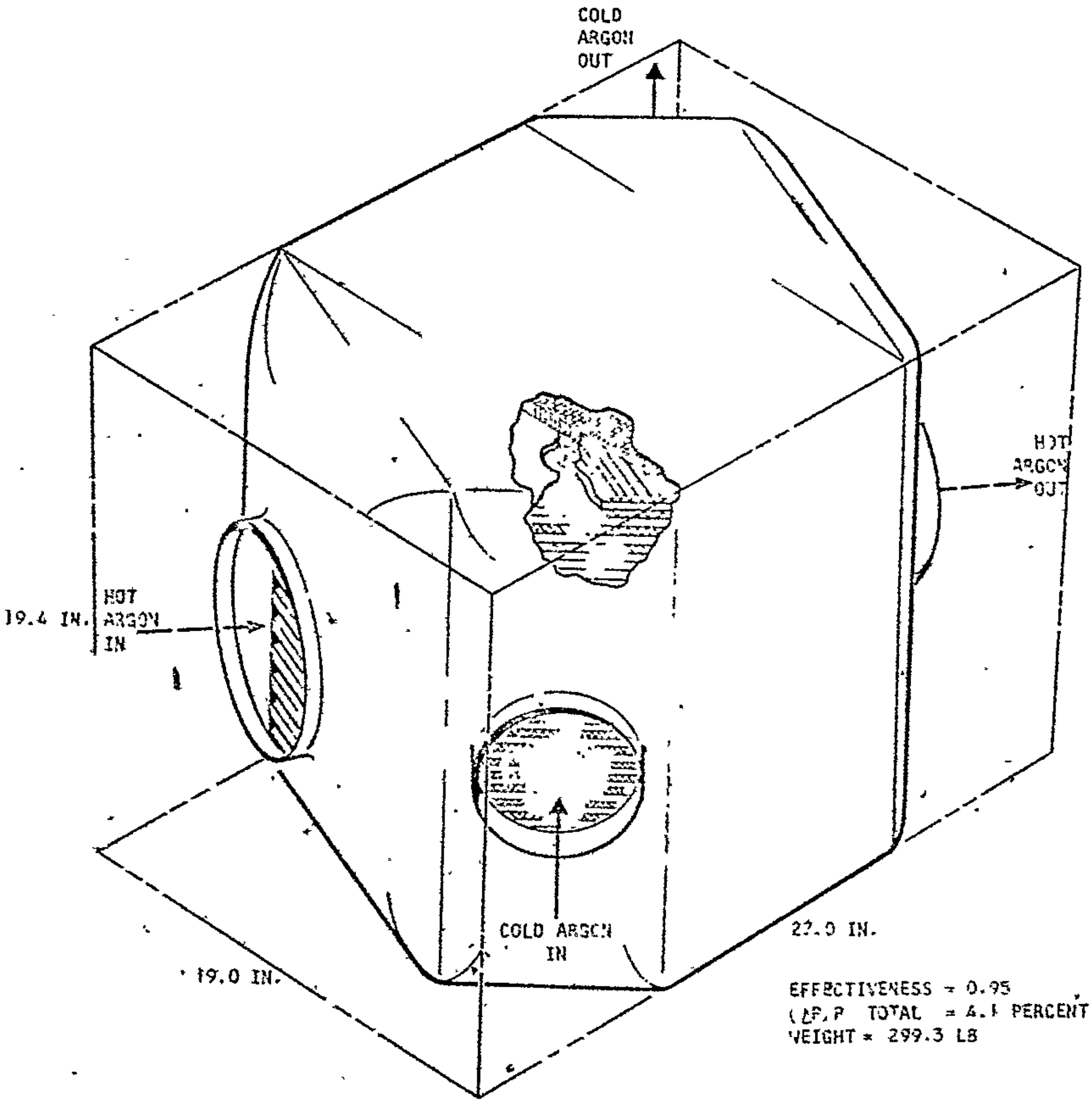

Figure 26. Typical Plate-Fin Pure Counterflow
Heat Exchanger

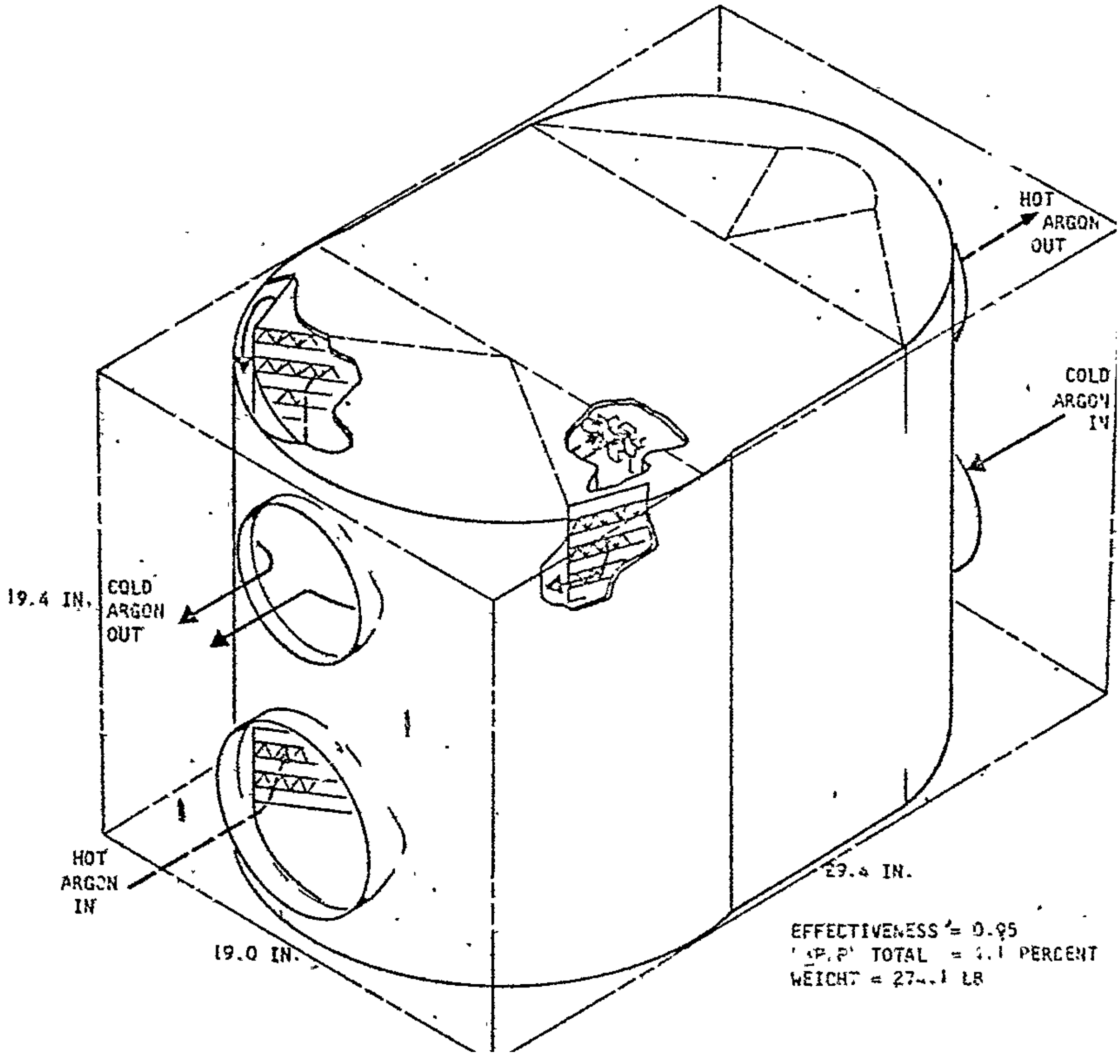

Figure 27. Alternate Packaging of Plate-Fin Pure Counterflow Heat Exchanger

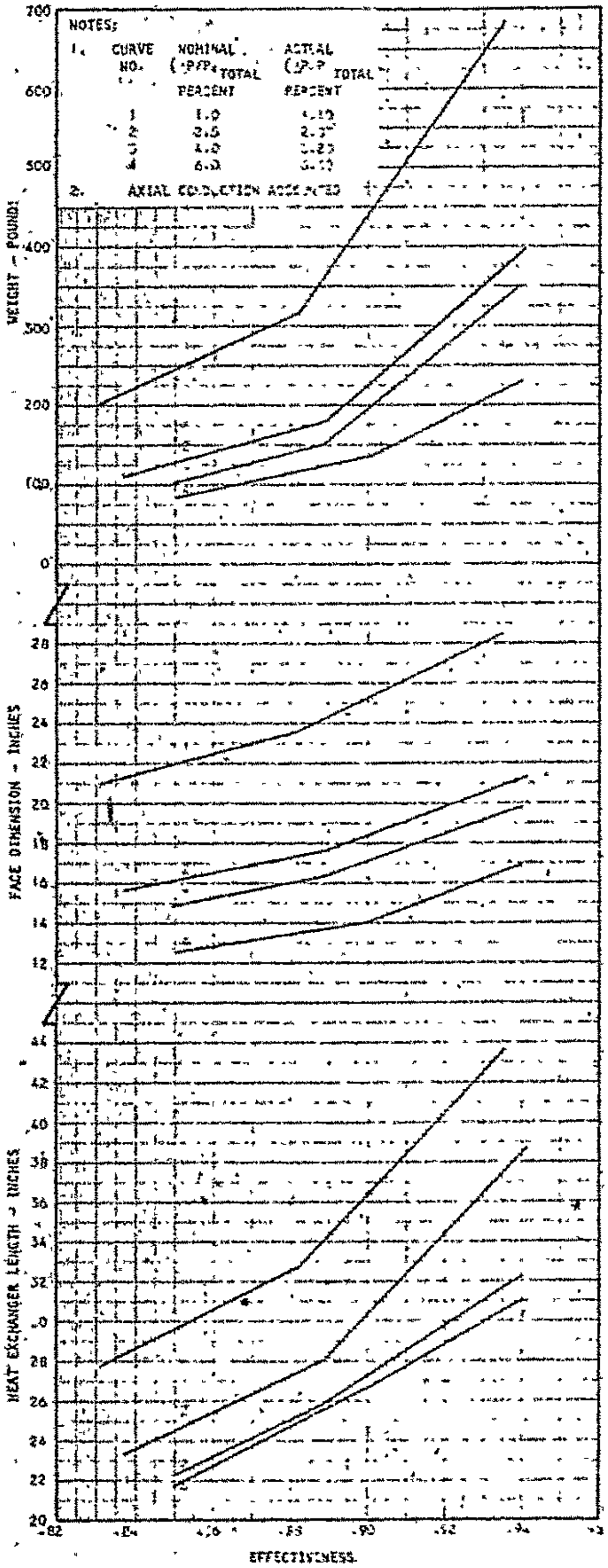

Figure 28. Plate-Fin Pure Counterflow Heat Exchanger Parameters Versus Effectiveness

package coupled with reasonable dimensions. An examination of the heat transfer cores originally designed by the computer programs eliminated the multi-pass cross-counterflow plate fin heat exchanger from further consideration. This elimination was possible on the grounds that not only was this type of core much heavier than the other types considered, at all operating conditions, but it was also the most complex to package. Having eliminated this particular type, careful consideration was given to packaging concepts for each of the other three types. In the case of both the pure counterflow and the cross counterflow tubular matrices multiple concentric ring packaging was selected as optimum. This type of packaging is illustrated in Figures 11, 11A and 21. With the pure counterflow plate and fin heat exchangers the choice of manifolding and packaging was more limited and the double triangular transition sections illustrated in Figure 27 were selected as optimum.

In order to obtain the isometric diagrams, heat exchanger weights and dimensions used throughout this report at least one layout drawing was made of each of the concepts considered for each type of heat exchanger. As stated previously, there is no simple, unique heat exchanger concept or type which is most satisfactory at all conditions. For the range of problem conditions examined, that is, effectiveness from 0.75 to 0.95 and pressure drop ratio $(\Delta P/P)_{TOTAL}$ from 1 percent to 8 percent a very rough guide in the selection of the optimum cores may be made as follows. At the highest effectiveness and lowest pressure drop conditions pure counterflow tubular heat exchangers present the lightest weight solutions. If minimum projected area is more valuable than minimum weight, pure counterflow plate-fin cores may be used, but at a considerable weight penalty. In the intermediate range pure counterflow plate-fin solutions yield both minimum weight and minimum projected area. At the low effectiveness and high pressure drop section of the range cross-counterflow tubular units have the lightest weights, but projected areas may be reduced by the selection of pure counterflow plate-fi units.

Figures 29 and 30 have been prepared to compare in detail the three types of heat exchangers which are being considered for use in the Brayton cycle system. These two figures were prepared by carefully considering the information presented in Figures 12, 22 and 28. As the exact pressure drop values used in each of these figures do not coincide a slight amount of interpolation was required. The interpolations were based on the very large mass of data obtained by AiResearch while formulating these designs. In Figure 29 the heat exchangers are compared on the basis of weights and smallest projected area that the heat exchanger presents from any particular side. The three sets of curves are for three different total percent pressure drops. From these curves another set of curves, Figure 30, has been prepared which presents the selected minimum weight and minimum projected area designs for the given problem statement range.

In summary, Figure 30 presents the recommended recuperator designs which should be considered when making a selection for the Brayton cycle system. If the NASA selected system conditions do not coincide with the actual data points, the curves may be interpolated to obtain approximate solutions. Since this process does not yield an exact solution, reevaluation of the heat exchanger parameters should be undertaken to determine final design details for the operating condition selected.

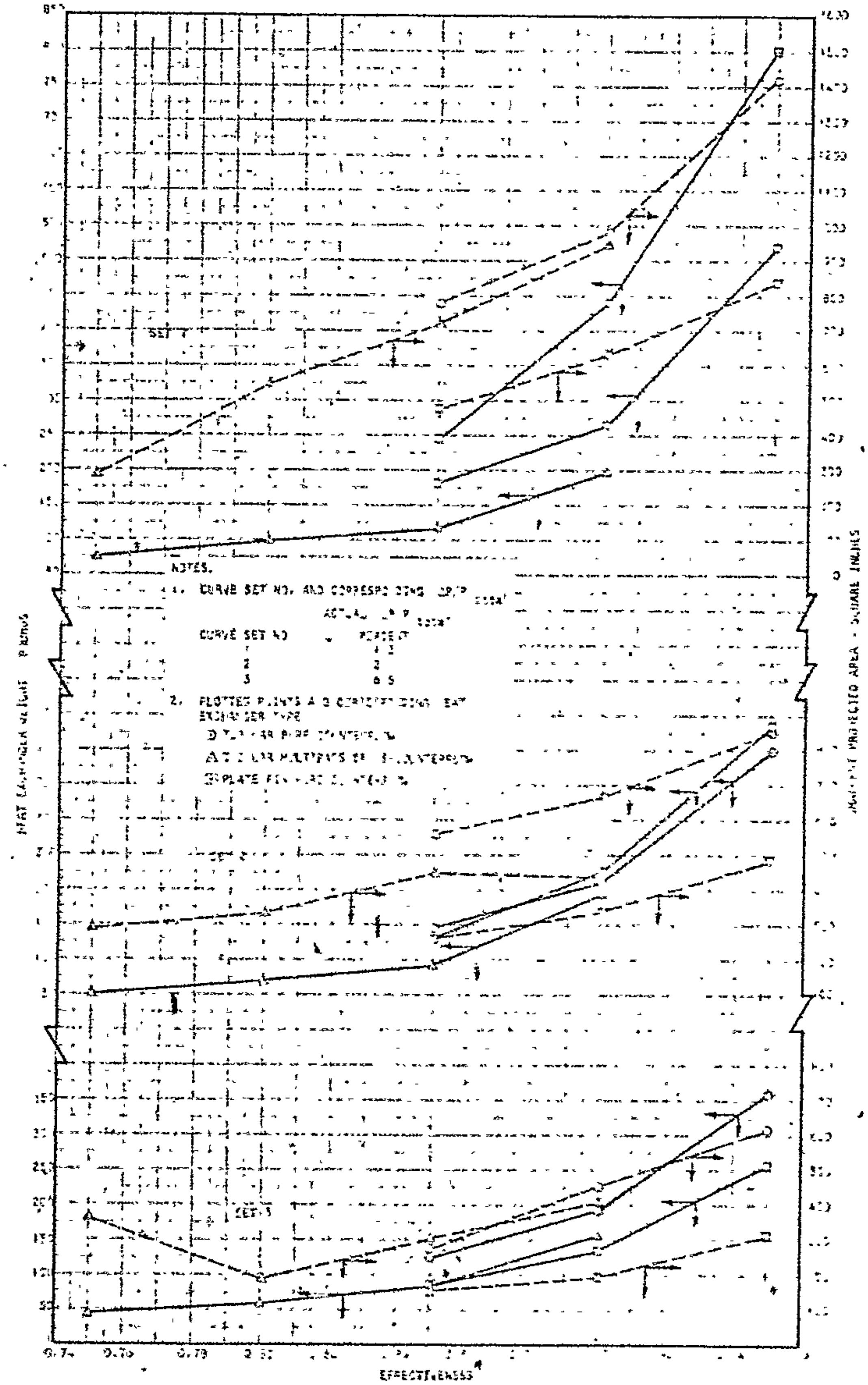

Figure 29 Heat Exchanger Weights and Projected Areas For Three Matrix Types

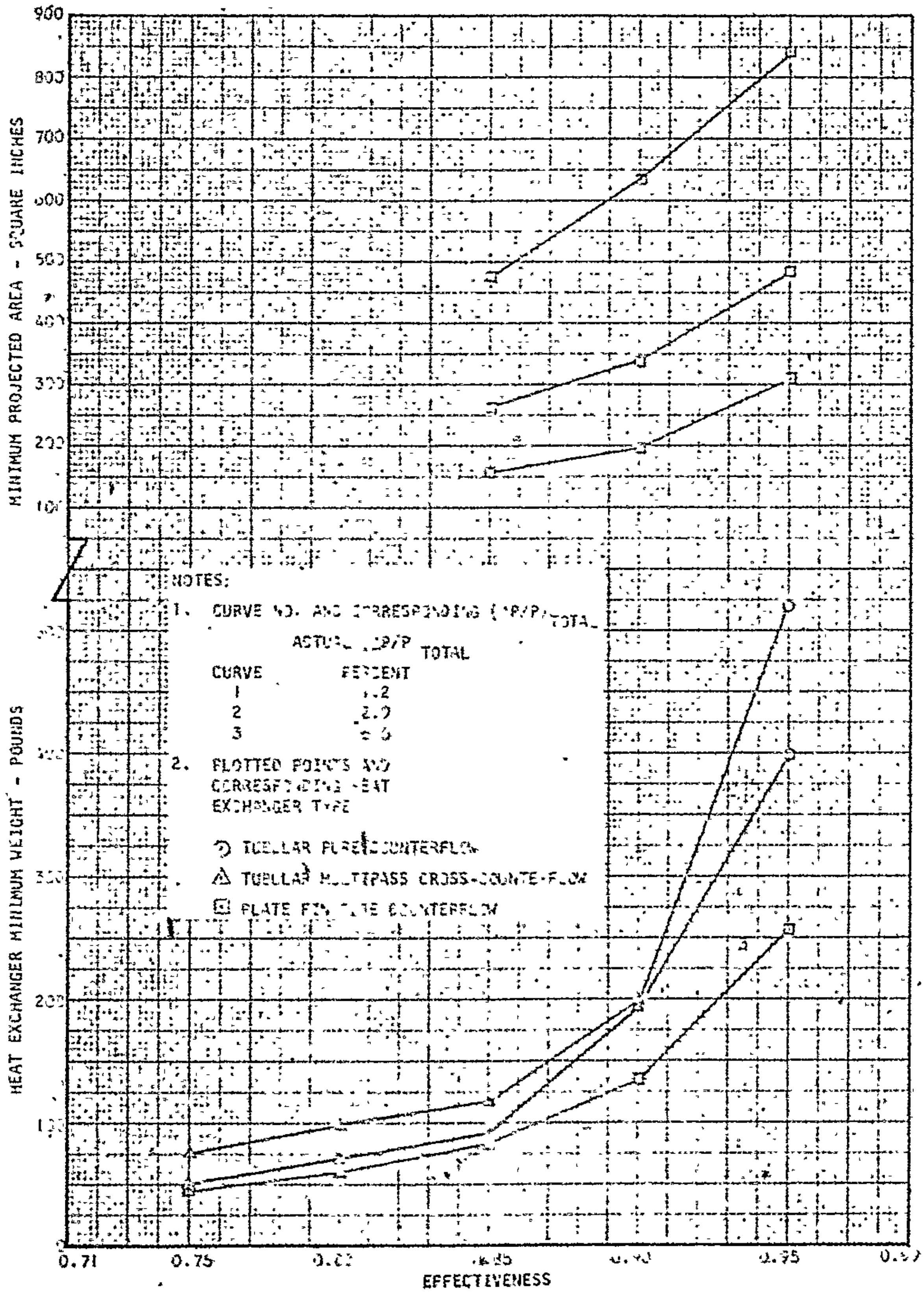

Figure 30. Heat Exchanger Minimum Weights and Minimum Projected Areas for Brayton Cycle Application

REFERENCES

AiResearch Report L-3895 Vo. I, Rev. 1, "Recuperator Development Program, for a Solar Brayton Cycle System," August 19, 1963. (NASA RFP:APGO-1527)

2. H. W. Hahnemann, "Approximate Calculation of Thermal Ratios in Heat Exchangers Including Heat Conduction in Direction of Flow," National Gas Turbine Establishment Memo No. M36, 1948 also available from the Defense Documentation Center as ATI 74031.

3. G. D. Bahnke and C. P. Howard, "The Effect of Longitudianl Heat Conduction on Pericdic - Flow Heat Exchanger Performance," Paper No. 63-AHGT-16, ASME, 1963.

4. W. M. Kays and A. L. London, Compact Heat Exchangers, McGraw-Hill, 1958

5. E. M. Sparrow and A. L. Loeffler, "Longitudinal Laminar Flow Between Cylinders Arranged in Regular Array," A. I. Ch. E. Journal, Vol. 5, Sept. 1959, pp. 325-330.

6. L. D. Palmer and L. L. Swanson, "Measurements of Heat-Transfer Coefficients, Friction Factors, and Velocity Profiles for Air Flowing Parallel to Closely Spaced Rods." International Developments in Heat Transfer, ASME, 1961

7. "Heat Transfer during Longitudinal Flow of Water around Bundle of Rods. with Relative Pitch of s/d = 1.4." Inzhenerno - Fizicheskii Zhurnal (Russian), v. 4, n. 3, March 1961, p. 3-9.

8. H. Kattchee and W. V. Mackewicz, "Heat-Transfer and Fluid Friction Characteristics of Tube Clusters With Boundary-Layer Turbulence Promoters," Paper No. 63-HT-1, ASME, 1963.

9. M. V. Mackewicz, "Experimental Investigation of Fluid Flow Characteristics of Pin-Type Fuel Elements" paper presented at the American Nuclear Society Meeting, San Francisco, Dec. 1960).

10. B. W. LeTourneau et al "Pressure Drop Through Parallel Rod Subassemblies Having a 1.12 Equilateral Triangular Pitch", Report No. WAPD-TH-118, Westinghouse, 1955.

APPENDIX A

SMALL SCALE TEST PROGRAM
RECUPERATOR DEVELOPMENT PROGRAM
SOLAR BRAYTON CYCLE SYSTEM

In the original proposal for the recuperator development program, AiResearch Report L-3595, Rev. 1, Volume 1, a small scale test program was proposed. The purpose of this small scale test program was to obtain data which would confirm the results of the analytical procedures utilized to design the heat exchangers. Particular emphasis was made at the time of the proposal on tests to evaluate the effects of longitudinal heat conduction in pure counterflow heat exchangers. Also mentioned at this time was the possibility of running tests to obtain data on both nonuniformity o flow distribution and basic heat transfer and pressure drop data for flow outside and parallel to, tube bundles.

As a result of the work so far completed in the recuperator development program it has become necessary to revise and update the original proposed small scale test program. The purpose of this report is, therefore, to outline the actual small scale tests which will be conducted during the second three months of the study program. The same three categories of testing, that is, axial conduction, flow distribution and basic heat transfer data will still be conducted, however the details of the testing in each of these categories has been revised.

AXIAL CONDUCTION

It has been pointed out previously that axial conduction can have a severe detrimental effect on pure counterflow heat exchangers where high effectiveness is required. At the time when the original proposal was written there was no adequate means of allowing for this effect, available. Two analytical methods of treating this problem had been derived at AiResear and these were presented in Appendix D of the above mentioned AiResearch report. No confirmation of these analytical methods was at that time available. It was proposed that some small scale tests be conducted to verify the results of this analytical treatment. The tests proposed were that a tube in a tube in a heat exchanger be constructed and run as a high effectiveness recuperator. The material and material thicknesses of the inner tube wall would be varied, thus enabling very substantial differences in axial conduction to be investigated.

Since the time of the proposal not only has AiResearch devoted considerable additional time to the analytical investigation of the problem of axial conduction, but the work of other investigators in this field has become available. The two main sources of other information were from papers of Bahnke and Howard and of Hahnemann. The results obtained by both of these investigators (References 1 and 2) yield identical results to the revised AiResearch approach to the problem of axial conduction. The revised AiResearch method was presented in a previous progress report (Reference 3). With the additional AiResearch effort and the confirmation available from these other sources AiResearch now feels that the previously proposed axial conduction tests are unnecessary and that the current analytical techniques are satisfactory.

In the pure counterflow heat exchanger designs where the metal conduction path is completely defined, no additional effort is required in the field of axial conduction. With the plate and fin heat exchangers however, a problem still exists. The definition of the metal conduction area and of the true thermal conductivity of the matrix is not fully defined. The tube plate, side plate and header bar metal conduction areas are defined, however, the effect of the fins, particularly the offset type of fins, is not so easily determined. With offset fins there is no continuous path for heat conduction down through the actual finned area. The part of the fin that is brazed to the plates does contribute some additional cross-sectional area to the path for heat conduction. Just how much this cross-sectional area affects the amount of heat conduction is not fully known. In addition, as in many of the heat exchangers the fins are of a different material than the plate (nickel fins and steel plates). The exact metal conductivity of the fin-to-plate braze joint is not fully known. It is, therefore, proposed that a series of small scale tests be conducted to determine the effective conductivity area of plate-fin cores. A small plate and fin sample will be fabricated utilizing the type of fins and materials that are being considered for the Brayton cycle recuperator. The quantity to be determined from these tests is the product of the thermal conductivity and the cross-sectional area (KA). This quantity is best defined by the following equation

$$KA = L \times \dot{Q}/\Delta T$$

where $\dot{Q}$ = heat transferred

L = conduction path length

ΔT = temperature difference (hot end to cold end)

The KA factor for the fabricated samples will be determined by measuring the overall electrical resistivity of the plate and fin specimen. From this measured electrical conductance it will then be possible to determine the thermal conductance by use of the Lorenz number.

FLOW DISTRIBUTION

From the results of the parametric analysis one of the heat exchanger matrices of prime interest will be the pure counterflow plate and fin type. The overall configuration of this type of heat exchanger, which requires triangular shaped pieces on either end of the core to permit access and egress of the fluids has been discussed in some detail in previous reports. Owing to this requirement for offsetting the flow direction from the face of the heat exchanger core, it is possible that some nonuniformity in flow distribution will occur within the core. In very high effectiveness heat exchangers it is possible that this nonuniformity in flow distribution could have a detrimental effect on heat exchanger performance. While the effect of nonuniformity in flow distribution on heat exchanger performance is subject to reliable analytical techniques, the estimation of the actual nonuniformity is less easily estimated. In order to ensure that no real loss in performance occurs due to flow maldistribution in a final design, plate and fin counterflow heat exchanger, a series of small scale tests are proposed.

A fluid distribution test section will be fabricated from layers of both the hot and cold side fins. The test section will include the inlet and outlet triangular sections with the selected loose fins within them and will also include representative headers to feed each of the layers within the test section. The simulation of the overall configuration is necessary as both the inlet and outlet manifolds and the inlet and outlet triangular sections may exert a considerable influence on the flow distribution. Flow distribution will be measured by recording a series of pressures and pressure drops across the width of the heat exchanger. A typical test section, together with the type of instrumentation which would be utilized, is shown in Figure 1. Actual distribution would be measured in both passages. A considerable amount of previous experience obtained by AiResearch in the field of flow distribution has shown clearly that flow distribution is a function of geometry only and is not affected in any way by any of the conventional flow parameters. With the overall design concept being considered for these plate and fin cores which utilize approximately 80 to 90 percent of the available overall pressure drop within the heat exchanger core, no serious problems are anticipated with flow distribution.

BASIC HEAT TRANSFER DATA FOR TUBULAR MATRICES

One of the matrices which has been considered throughout the parametric analysis has been a pure counterflow tubular heat exchanger. Two main problems existed in the examination of this type of matrix. At the time of the proposal, AiResearch did not have a rapid and accurate means of designing this type of matrix for a given application. Also, there is little information available on either the heat transfer or pressure drop

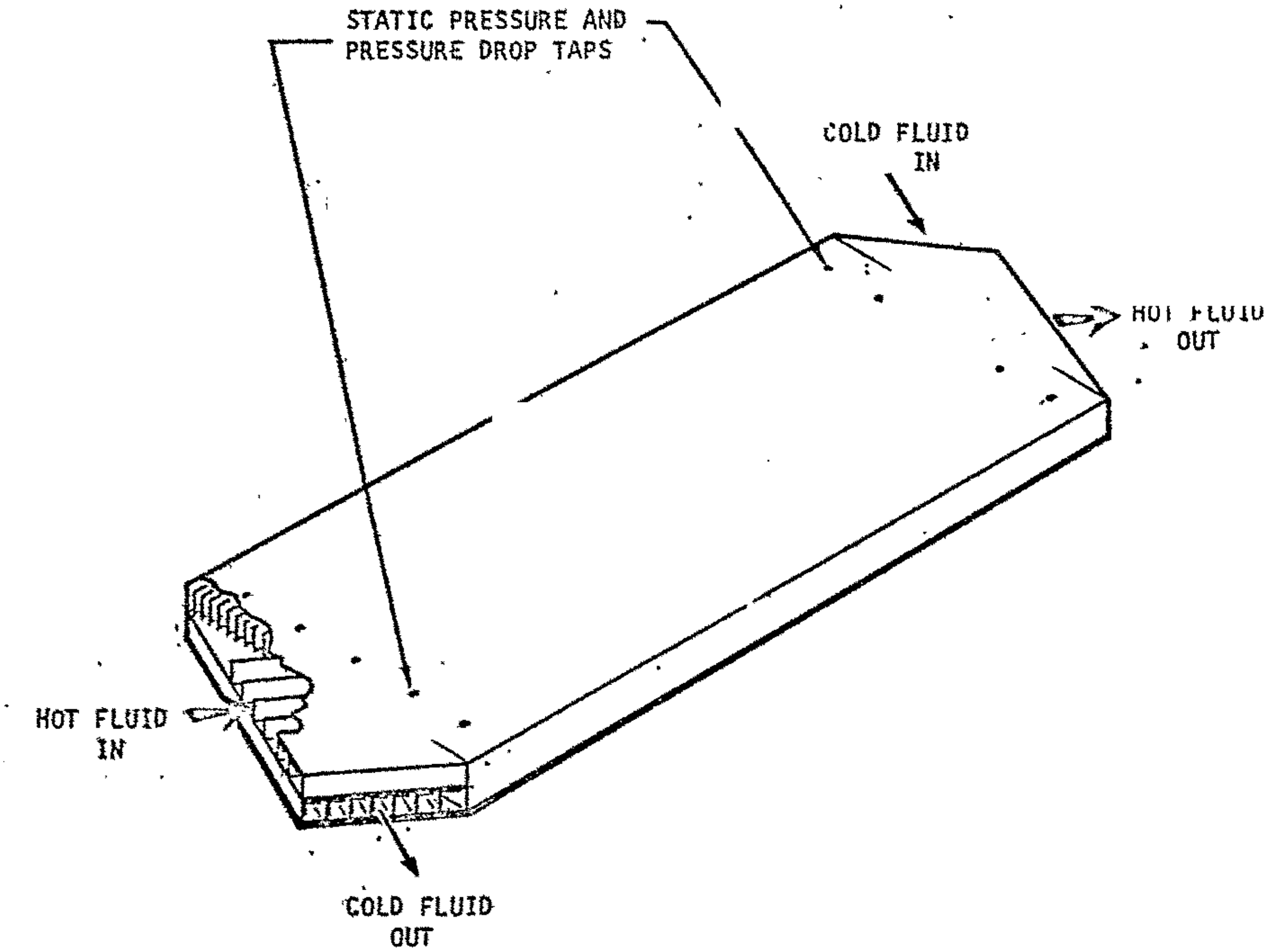

A-4226

Figure 1. Typical Flow Distribution Test Unit

characteristics of flow outside of and parallel to tube bundles. The little data that is available on these characteristics is limited almost entirely to the turbulent flow regime. In the recuperator designs contemplated for Brayton cycle applications the flow regime within the heat exchanger will almost certainly be laminar.

Throughout the parametric analysis considerable effort has been expended in eliminating both these drawbacks to investigating the pure counterflow tubular matrix. A program has been written for the IBM 7074 digital computer which permits the rapid and accurate designing of this type of heat exchanger. This program includes the effect of axial conduction. In an effort to obtain the required basic heat transfer and pressure drop data, an extensive literature survey was conducted. As mentioned above, this survey was not too successful as little data was found in the appropriate operating range. During the parametric analysis, therefore, the data used for outside the tube bundle has been based on estimated values. Investigations were conducted to determine the effect on heat exchanger size of varying these basic characteristics. The results of these investigations, together with the most suitable designs determined, will be shown in the final parametric analysis report.

In the highest effectiveness and lowest pressure drop section of the range of conditions being considered by this parametric analysis, the pure counterflow tubular heat exchangers show promise. It is desirable to obtain confirmation of the designs by obtaining more reliable basic data. It is, therefore, proposed that a small test section be built utilizing the tube size and spacing shown to the most suitable by the parametric analysis.

In order to obtain suitable data from a minimum expenditure test setup, careful consideration must be given to the design of the test core. The test core which will be built will contain a tube bundle which would be arranged in a rectangular bundle with a high aspect ratio.

The tube length will be at least 3 feet. These overall dimensions are basic to the requirement of obtaining satisfactory data. A reasonable number of tubes is required to ensure that end and edge effects do not distort the results. The rectangular configuration with the high aspect ratio will ensure that the flow on the outside of the tubes can be introduced and removed from the tube bundle with minimum end effects. The long tube length will also ensure that a fully established flow regime exists throughout the heat transfer matrix. The tests will be conducted by flowing air across the outside of the tubes and water through the tubes. High water flow rates would be utilized to minimize the effect of water side characteristics on overall performance. The overall test setup configuration and instrumentation which will be utilized are typical of the many hundreds of this type of tests which have been previously conducted by AiResearch.

REFERENCES

1. G. D. Bahnke and C. P. Howard, "The Effect of Longitudinal Heat Conduction on Periodic-Flow Heat Exchanger Performance," Paper No. 63 - AHGT - 16, ASME, 1963

2. H. W. Hahnemann, "Approximate Calculation of Thermal Ratios in Heat Exchangers Including Heat Conduction in Direction of Flow," National Gas Turbine Establishment Memo No. M36, 1948 also available from Defense Documentation Center as ATI 74031

3. AiResearch Report L-9370, "Recuperator Development Program, Solar Brayton Cycle System, Progress Report for January 1964"

N 66-17325
(ACCESSION NUMBER)
~~48~~ 63
(PAGES)
CR 70381
(NASA CR OR TMX OR AD NUMBER)

(THRU)
NONE
(CODE)
03
(CATEGORY)

AIRESEARCH MANUFACTURING COMPANY

A DIVISION OF THE GARRETT CORPORATION

9851-9951 SEPULVEDA BLVD. • LOS ANGELES, CALIFORNIA 90009

TELEPHONE SPRING 6-1010, ORCHARD 0-0131 • CABLE: GARRETTAIR LOS ANGELES

3544 3/5

63

28053
2/26/66
1 copy

1 STOCK LOCATION	2 DATE RECEIVED YR 74 MO 2 DAY 22	12 SCREEN: OBTAIN BETTER COPY / OBTAIN AUTHORITY / REJECT / OUT OF PRINT SOD / ERRATA	17 ACCESSION NUMBER N 66-17325
3 RECEIPT TYPE & FORMAT: LOAN / LAST COPY / [X] PC / MF / 35 MM / 16 MM / MAGNETIC TAPE / CARDS / OTHER (BOX 16)		13A ANNOUNCEMENT VOL 74 ISSUE 07; 13B FAS YES / [X] NO; GRA / WGA / [X] UNLAWN	18 PAGES 62; 19 SHEETS —; 20 LOW LIMIT PC MF; 21 SUBSCRIPTION
4 STOCK RECEIVED FOR SALE PC 0 MF	5 LOAN ETC DUE OUT RET	14 REPRODUCTION INSTRUCTIONS BLOWBACK; MAKE MICROFICHE YES / [X] NO	22 PRICES U UNIT / E PC + MN BOX 16; 6.25; [X] P PC; M MN; WI; [X] DEMAND
6 TRANSACTION NEW ITEM [X] / DUPE / SUPERSEDES / PRIOR NUMBER		PRINT NO: 1, 4, 7; 1 UP: (2), 5, 8; 2 UP: 3, 6, 9; MIX / SAME SIZE / ORDER STOCK FROM; 15 PRESTOCK: PC DUE IN / PC PRINT / PC SOURCE TO ORDER / MF PRINT CODE 0	23 CATEGORY —; 24 DISTR CODE —; 25 INITIALS ACC A RM; 11 NOT FULLY LEGIBLE [X] COLOR
7			26 FILL FROM PAPER COPY ETC BX; MICRO-NEGATIVE XM; 27 PUBLIC RELEASABILITY T
8 REPORT NUMBERS (XREF) NASA-CR-70381		16 REMARKS	
9 RELATED-DOCUMENT			
10 CONTRACTING OFFICE-BILLING CODE NASA -100			
28 FORM, PRICE, ETC. 1200	29 ANN CODE 0000		

1 ARCHIVES 2/25

FORM NTIS-77
(REV. 1-73)
USCOMM-DC 11954-P73

U.S. DEPARTMENT OF COMMERCE
NATIONAL TECHNICAL INFORMATION SERVICE

DOCUMENT TRAVELER